International Journal of Cognitive Computing in Engineering 6 (2025) 552–568

Contents lists available at ScienceDirect

International Journal of Cognitive Computing in Engineering

journal homepage: www.keaipublishing.com/en/journals/international-journal-of-cognitive-computing-in-engineering/

# Normalized SPSA for Hammerstein model identification of twin rotor and electro-mechanical positioning systems

Nik Mohd Zaitul Akmal Mustapha, Mohd Ashraf Ahmad *

*Faculty of Electrical and Electronics Engineering Technology, Universiti Malaysia Pahang Al-Sultan Abdullah, 26600 Pekan, Pahang, Malaysia*

ARTICLE INFO

*Keywords:*
System identification
Hammerstein model
Optimization
SPSA
Continuous-time
Metaheuristic approach

ABSTRACT

A wide range of optimization methodologies have been introduced for identifying Hammerstein model systems, but existing approaches often face challenges such as convergence instability, computational inefficiency, and over-parameterization. These issues necessitate research into fast, stable, and precise identification methods. This study proposes the normalized simultaneous perturbation stochastic approximation (N-SPSA) to address the challenges mentioned earlier. The N-SPSA mitigates unstable convergence and excessive parameter growth of the conventional SPSA by normalizing objective functions to their highest value, ensuring stable convergence while maintaining the same number of coefficients. The effectiveness of the proposed method was validated by modeling the actual systems, which included the twin-rotor system (TRS) and the electro-mechanical positioning system (EMPS). Performance metrics such as the objective functions statistics, the number of function evaluations (NFE), and time- and frequency-domain responses were used for evaluation. For the TRS, the N-SPSA improved the mean objective function by 18.09 % compared to the average multi-verse optimizer sine-cosine algorithm (AMVO-SCA) and 3.42 % compared to the norm-limited (NL-SPSA), while reducing the computational load by 60 % compared to the AMVO-SCA. Similarly, for the EMPS, the N-SPSA improved the mean objective function by 71.19 % over the NL-SPSA and 25.18 % over the AMVO-SCA, achieving a 50 % reduction in computational effort compared to the AMVO-SCA. Additionally, Wilcoxon's rank-sum test results for both the TRS and EMPS confirmed the statistical superiority of the N-SPSA over the NL-SPSA. These findings demonstrate that the N-SPSA provides a fast and precise solution for the identification of continuous-time Hammerstein systems, overcoming the limitations of existing methods.

## 1. Introduction

System identification has been classified as a dynamic model estimation method for actual plants. Identification techniques also offer effective modeling of complex plants owing to their compatibility and robustness in addressing nonlinear systems such as Unmanned Aerial Vehicles (UAVs) (Ramachandran & Sangaiah, 2021), power distribution systems (Gogula & Vakula, 2024), and crane systems (Saat et al., 2025). There are five principal techniques comprising the modular layouts of state-space models (Haber & Verhaegen, 2020; X. Liu & Yang, 2022; Masti & Bemporad, 2021), neural networks (Aji et al., 2020; L. Liu et al., 2023; Misyris et al., 2020), block-oriented models (Baldelli & Lind, 2005; Gómez & Baeyens, 2004; Zimmerschied & Isermann, 2009), Volterra (Fard et al., 2005; Hacioğlu & Williamson, 2001; Janjanam et al., 2021) series models, and structures that embedded the nonlinear autoregressive moving averages with exogenous input (NARMAX) (He et al., 2015; H. L. Shi et al., 2006; Yan & Deller, 2016). Among these, artificial neural networks (ANNs), are notable for their versatility and ability to handle noisy and complex datasets (Sharma et al., 2021) . Their adaptability makes them particularly suitable for system identification, especially in addressing nonlinearities and challenging environments.

Block-oriented models, however, remain highly preferred by the research community because they have a simple structure that eases both apprehension and utilization (M. Schoukens & Tiels, 2017). They also provide a broad generalization of nonlinear systems, improving real-time applicability (J. Schoukens et al., 2015). Block-oriented models can be divided into Hammerstein, Wiener, and Hammerstein-Weiner. The Hammerstein model contains a sequential network of nonlinear functions and linear dynamic subsystems. In contrast, the Wiener model comprises a sequential network of linear dynamic and static nonlinear subsystems. Meanwhile, the Hammerstein-Weiner model centralizes a linear dynamic sub-plant

* Corresponding author.
*E-mail address:* mashraf@umpsa.edu.my (M.A. Ahmad).

https://doi.org/10.1016/j.ijcce.2025.04.004
Received 14 September 2023; Received in revised form 21 April 2025; Accepted 22 April 2025
Available online 26 April 2025

**Nomenclature**

| | |
|---|---|
| UAVs | Unmanned aerial vehicles |
| ANNs | Artificial neural networks |
| SPSA | Simultaneous perturbation stochastic approximation |
| N-SPSA | Normalized SPSA |
| NL-SPSA | Norm-limited SPSA |
| AMVO-SCA | Average multi-verse optimizer sine-cosine algorithm |
| NFE | Number of function evaluations |
| TRS | Twin-rotor system |
| EMPS | Electro-mechanical positioning system |
| PMAs | Pneumatic muscle actuators |
| IRC | Isometric recruitment curve |
| APAs | Amplified piezoelectric actuators |
| GA | Genetic algorithm |
| PSO | Particle swarm optimization |
| ARMAX | Autoregressive moving average with exogenous inputs |
| FLANN | Functional link artificial neural network |
| IIR | Infinite impulse response |
| CSA | Cuckoo search algorithm |
| DE | Differential evolution |
| FIR-MA | Finite impulse moving average |
| DEA | Differential evolution algorithm |
| BBO | Biogeography-based optimization |
| BFO | Bacterial foraging optimisation |
| BSA | Backtracking search algorithm |
| OCBO | Orthogonal colliding bodies optimisation |
| CRPSO | Craziness based PSO |
| ABC | Artificial ant colony |
| CSSA | Chaotic salp swarm algorithm |
| RF | Radio frequency |
| WSNs | Wireless sensor networks |
| GK-SPSA | Knowledge-informed historical gradient-based SPSA |
| ANN | Artificial neural network |
| W-SPSA | Weighted-SPSA |
| PCA | Principal components analysis |
| PC-SPSA | Principal components SPSA |
| c-SPSA | Cluster-wide SPSA |
| OD | Origin-destination |
| DTA | Dynamic traffic assignments |
| SISO | Single-input-single-output |
| PSD | Power-spectral density |
| MIMO | Multi-input multi-output |

between a series of paired or multiple nonlinear subsystems. Comparatively, the Hammerstein model is more popular than the others owing to its precise model estimation using fewer parametric elements. Apart from being more simplistic in actual application, the polynomial representation for nonlinear models is more flexible (Ozer et al., 2016). Moreover, the well-defined layout of a Hammerstein model renders it suitable to use varying estimation approaches throughout individual blocks (Mehmood et al., 2020). Recent advancements in the Hammerstein model identifications, such as improved optimization techniques, have further enhanced its effectiveness in nonlinear system identification, making it an essential tool in modern applications.(Islam et al., 2024).

On the other hand, simultaneous perturbation stochastic approximation (SPSA) is a potential tool for identifying continuous-time Hammerstein models due to its effectiveness in tuning high-dimensional problems with less computational time. Despite these significant merits, the standard SPSA still faces challenges of convergence instability and design parameter overgrowth when applied to continuous-time Hammerstein models. These limitations hinder the accuracy and reliability of model identification for nonlinear dynamic systems, especially in real-world applications requiring robustness and efficiency. Addressing these challenges is essential for obtaining stable convergence, thus improving model precision. Motivated by these challenges, this research aims to overcome the inherent limitations of the conventional SPSA algorithm by introducing the normalized SPSA (N-SPSA).

The proposed N-SPSA algorithm offers significant advantages in addressing convergence instability issues, ensuring precise and reliable performance. By normalizing measured objective functions to their highest value, the gradient estimation process is computed based on two normalized objective functions. This approach effectively prevents excessive growth in updated design variables while maintaining the same number of coefficients as the standard SPSA. Hence, the ability of the N-SPSA to precisely estimate both linear and nonlinear subsystem structures of the continuous-time Hammerstein model is enhanced. Specifically, the incorporation of the normalized function improves the statistical performances of the objective function, the number of function evaluations (NFE), Wilcoxon's rank test, and the time and frequency-domain responses of the twin-rotor system (TRS) and the electro-mechanical positioning system (EMPS). Furthermore, this study also conducts a performance comparison between the proposed N-SPSA and other established algorithms, such as conventional SPSA, norm-limited SPSA (NL-SPSA), and the average multi-verse optimizer sine-cosine algorithm (AMVO-SCA). The key contributions of this study are outlined as follows:

i. The proposed N-SPSA addresses the limitation of conventional SPSA in overcoming the unstable convergence issue by utilizing two normalized functions for gradient estimation, which can effectively control variable growth while maintaining the same number of coefficients
ii. The proposed N-SPSA algorithm achieves heightened accuracy in model identification with fewer function evaluations per iteration, reducing computational load. This efficiency supersedes the performance of multi-agent-based optimization techniques.
iii. This is the first time the N-SPSA was applied to a continuous-time Hammerstein model framework and compared with other recent algorithms. This comparison effectively demonstrated the algorithm's precision in replicating the parametric components of an actual system.
iv. The Hammerstein model framework introduced in this study independently determines parametric components for nonlinear and linear subsystems. This approach mitigates over-parameterization issues, leading to a comparatively smaller computational load while ensuring robust model identification.

This paper is divided into six main sections. Following the introduction in Section 1, Section 2 presents an extensive literature review comprising a wide range of optimization methodologies employed for the identification of Hammerstein model systems. Section 3 describes the proposed formulation of the optimization problem according to the required model identification. Section 4 delineates the structural reviews between the conventional SPSA algorithm and the proposed N-SPSA algorithm. This section also explains in detail the layout and procedure for using the N-SPSA, addressing the formulated problem and identifying the Hammerstein model. In Section 5, the validity of the N-SPSA-based method is assessed against other preceding optimization approaches in terms of real-time identification of the practical plants. Finally, Section 6 concludes the study.

## 2. Literature review

To date, various real-time applications that employ Hammerstein systems, such as the cascaded tank benchmark systems (Aljamaan et al., 2021), are complicated due to many factors, such as voltage inputs to the pump and minor nonlinearities during measurements. These elements highly influence the nonlinear characteristics of such systems. Load dynamics in voltage management is also one of the issues of concern (Bao et al., 2018), where the slightest fluctuations in load dynamics can substantially affect voltage transient behavior. The study modeled both active and reactive power loads to determine their impact on voltage transients, demonstrating a highly nonlinear coupled dynamic system. Similar to many mechanical systems, the turntable servo system (Zhang et al., 2016) involves the influence of force (depending on both position and velocity) on mass movement. These forces behave nonlinearly in certain operational zones, such as Coulomb friction and dead zones. Such systems are also applied to regulating a quadratic DC/DC boost converter (Alonge et al., 2015). However, research has highlighted complicated calculations arising from the extra inductors and capacitors that increased the number of poles in the transfer function, resulting in nonlinear behavior concerning the duty cycle.

Pneumatic muscle actuators (PMAs) are widely utilized in the medical field, especially in robotic equipment for rehabilitation (X. Shi & Zhang, 2016). They exhibit substantial nonlinearity owing to their inherent features, including friction between the bladder and braid, slight deformation after each operation, and thermal effects. Many researchers have also explored electrically stimulated muscles (Le et al., 2012) for motor control analysis and developed neuroprosthetic motor systems, particularly inpatient rehabilitation programs. The static nonlinearity imitates the isometric recruitment curve (IRC), which shows the consistent relationship between the stimulus activation level and the steady-state output torque when the length of the muscle is fixed. Moreover, there is growing interest in using Hammerstein structures to mathematically model the hysteresis in amplified piezoelectric actuators (APAs) (Saleem et al., 2017). APAs have been applied in numerous control engineering disciplines, such as vibration suppression and precision positioning. Nevertheless, the main drawback of piezoelectric actuators is the nonlinear relationship between the applied voltage and the resulting displacement as a result of hysteresis and creep/drift effects.

Subsequent investigations in model identification have led to the rapid development of various methods, including iterative (Chidume & Djitté, 2013; G. Li & Wen, 2011; J. Li, 2013), over-parameterization (Jafari et al., 2014; Mao & Ding, 2016; Salhi & Kamoun, 2015), blind identification (Bai & Li, 2010), subspace (Hou et al., 2020), least square (F. Ding, X. Liu, 2013; D. Wang & Zhang, 2015), hierarchical identification (Ding et al., 2018; D. Wang, 2016; D. Q. Wang et al., 2015), and stochastic (Mao & Ding, 2014). Despite these new multimodal solutions, issues regarding the accuracy of the identified Hammerstein system remain unanswered as the operated process evolved into a complex multidimensional optimization problem (D et al., 2018). Biological- and nature-inspired metaheuristic approaches were then widely studied to resolve both restricted and non-restricted issues across multiple engineering and technological domains. Essentially, the metaheuristic category was favored for model identification of Hammerstein systems, given its superior efficacy, precision, and rate of convergence compared to those of deterministic approaches (Raja et al., 2018). For example, several studies preferred the genetic algorithm (GA) (Akramizadeh et al., 2002; Hatanaka, 2001; Kumon et al., 2000) as the conventional metaheuristic optimization approach to identify a Hammerstein system. However, the method was exposed to the potential limitation of over-parameterization resulting from redundant gains within the nonlinear and linear subsystems.

The particle swarm optimizer (PSO) technique was then proposed to identify Hammerstein systems (Hammar et al., 2017). This method employed an autoregressive moving average with exogenous inputs (ARMAX) model with a key term separation approach within a discrete-time transfer function to calculate the fractional order of nonlinear and linear subsystems. Further advancement in model estimation involved a functional link artificial neural network (FLANN) and an adaptive infinite impulse response (IIR) filter via the proposed implementation of the cuckoo search algorithm (CSA) (Gotmare et al., 2015). Compared to both PSO and differential evolution (DE), the linear subsystem comprised discrete-time transfer functions and recorded overshadowing identifying precision. Likewise, the gravitational search algorithm (GSA) incorporated the finite impulse moving average (FIR-MA) as a linear subsystem in identifying Hammerstein models (Xu et al., 2020). While the statistical results of GSA showed superior estimation competence in parametric components compared to that of the PSO technique, the method still suffered from over-parameterization from existing redundant gains within both linear and nonlinear subsystems. Other alternative metaheuristic algorithms have been simultaneously exemplified to identify Hammerstein systems including differential evolution algorithm (DEA) (Mete et al., 2016), biogeography-based optimization (BBO) algorithm (Yang & Jin, 2017), bacterial foraging optimization (BFO) algorithm (Pal et al., 2016a), backtracking search algorithm (BSA) (Mehmood et al., 2019), orthogonal colliding bodies optimization (OCBO) (Panda & Pani, 2016), craziness based PSO (CRPSO) algorithm (Pal et al., 2016b), artificial ant colony (ABC) (Zorlu et al., 2018), and chaotic salp swarm algorithm (CSSA) (Jin & Cui, 2020).

Many studies have also revealed other limitations that hamper the robustness of multi-agent-based optimization algorithms in Hammerstein system identification. Primarily, scholastic assessments of discrete-time models are widespread compared to the majority of real-time systems that instead advocate the continuous-time setting. Secondly, massive computation load is contributed by a multitude of unnecessary parametric components on the existence of redundant gains within the nonlinear subsystem. In regards to the propositioned composition of the computation interval for each iteration and the population size in most metaheuristic approaches, an extensive computation interval is required for convergence acquisition, describing the rigid nonlinear models with considerable dimensionality. Thus, ongoing research continues to explore the continuous-time Hammerstein system that fits parametric elements of a real-time structure. Further efforts were focused on preventing redundant nonlinear and linear parameters to control the computation weight in model identification. Researchers are more inclined to apply single-agent-based optimization for a smaller number of function appraisals within each iteration compared to its multi-agent counterpart.

A recent study applied the SPSA, a well-established single-agent-based optimization method developed by (James C Spall, 1992), for the Hammerstein identification system. This technique was chosen for its shorter computational time, suitability for tuning high-dimensional design parameters, and effective gradient approximation using only two measurements within the objective function. Remarkably, research has demonstrated the reliable performance of SPSA in overcoming various optimization issues across different engineering fields, including servo motor systems (Rădac et al., 2011), coupled well placement optimization (Pouladi et al., 2020), transportation problems (Ros-Roca et al., 2018), digital predistortion of radio frequency (RF) amplifier (Kelly & Zhu, 2018), dynamic demand calibration (Kostic et al., 2017) and wireless sensor networks (WSNs) (Azim et al., 2012). The enhanced practical compatibility of SPSA in various optimization challenges is achieved by exploiting its simple structure and ability to calibrate design variables using a wide range of dimensions at lower computation loads. In fact, SPSA can be further modified and tailored to integrate specific optimization tasks, showcasing its versatility. For example, knowledge-informed historical gradient-based SPSA (GK-SPSA) was developed according to historical gradient approximations as an updated SPSA variant to control the quality of medium voltage insulators (Kong et al., 2020). Other studies have assessed hybridization between

SPSA and artificial neural networks (ANN) to boost the search efficiency of conventional approaches (Abdulsadda & Iqbal, 2011). One study enhanced the weighted-SPSA (W-SPSA) to address extensive dimension problems and produced a marked performance in dynamic traffic assignments (DTA) (Antoniou et al., 2015). In another study, a novel algorithm called PC-SPSA was developed by integrating SPSA with principal components analysis (PCA) to improve the DTA calibration algorithm (Qurashi et al., 2020). The objective of the integration process is to minimize search noise, thus enhancing the scalability of SPSA for DTA model calibration. Besides, cluster-wise SPSA (c-SPSA) was proposed by dividing gradient approximation via simultaneous perturbation with small step sizes and homogeneous clustering to solve estimation issues in dynamic origin-destination (OD) modeling (Tympakianaki et al., 2015). This model was further advanced by (Tympakianaki et al., 2018) through the implementation of a robust SPSA algorithm to improve OD estimation. Their recent work focused on three innovative approaches to enhance the performance of SPSA algorithms in optimization and estimation tasks for OD problems: scaling variable updates (a novel technique for OD estimation), hybridizing analytical and stochastic gradient data in hybrid SPSA and c-SPSA versions, and evaluating new clustering criteria in c-SPSA.

Although SPSA-based methods are widely used to identify Hammerstein models, they record equivalent performance with other metaheuristic algorithms and suffer major operational limitations. In particular, the stability of yielded solutions from a conventional SPSA-based method may be compromised due to the continuous expansion of revised parameters throughout the parametric optimization of a Hammerstein system. An unclarified closed-form expression for the objective function in conventional algorithms was also identified to complicate the generation of a steady transfer function across all circumstances. Subsequent research implemented an NL-SPSA-based method to achieve convergence stability and solve previous shortcomings by employing a saturation function that restricts the revised control parameter (Ahmad et al., 2016). Nevertheless, the modified SPSA variant uses a pre-determined coefficient that limits its search capacity of the optimal control parameter, consequently diminishing its compatibility with specific model-free control problems. Hence, this impediment warrants alternative improvements to the conventional SPSA-based method to ensure convergence stability and superior parametric optimization.

Previous works (Ahmad et al., 2018; Mustapha et al., 2019) have expanded this framework and successfully applied N-SPSA to data-driven PID controllers for flexible joint manipulators and liquid slosh systems. Both studies found that model-free controller tuning using N-SPSA yielded more stable and greater control performance compared to other modified SPSA methods. Nevertheless, no studies have applied N-SPSA to identify continuous-time Hammerstein systems. Considering past literature studies, it is worth assessing the performance of N-SPSA in system identification for continuous-time Hammerstein systems.

## 3. Problem formulation

The undertaken procedure for model identification is described in this section. Fig. 1 comprises notations $g$, $H$ and $p := \frac{d}{dt}$ as the non-linear function, linear dynamic system and differential operator to collectively illustrate a single-input-single-output (SISO) continuous-time Hammerstein system. Both the input signal and output signal are perturbed by the noise signal $v(t)$, that are separately represented by notations $z(t)$ and $z'(t)$. The equation for output $z'(t)$ is conceivably expressed by:

$$z'(t) = H(p)g(u(t)) + v(t) \tag{1}$$

where

$$H(p) = \frac{B(p)}{A(p)} = \frac{b_l p^l + b_{l-1}p^l + \ldots + b_0}{p^m + a_{m-1}p^{m-1} + \ldots + a_0}, \tag{2}$$

with the output for the non-linear function is further expressed by:

$$g(u(t)) = \sum_{i=1}^{M} \delta_i \omega_i(u(t)) \tag{3}$$

where the notation $\omega(.)$ consists of a function of polynomial potential. The current procedure accounts for a set of pre-determined assumptions, including

**Assumption (1):** $m$, $l$ and $M$ are known,
**Assumption (2):** $a_i(i = 0, 1, \ldots, m-1)$, $b_i(i = 0, 1, \ldots, l-1)$ and $\delta_i(i = 1, \ldots, M)$ comprised of real numbers,
**Assumption (3):** Setting of $b_l = 1$ to individually acquire the values of $H(p)$ and $g(u(t))$,
**Assumption (4):** $g(0) = 0$.

The employed fitness function to appraise the proposed model is given by:

$$J(\overline{H}, \overline{g}) = \sum_{j=0}^{N} \left(z'(jt_s) - \overline{z}(jt_s)\right)^2 \tag{4}$$

where the sampling interval of $t_s$ is defined by $j = 0, 1, \ldots, N$ for $(u(t), z'(t))(t = 0, t_s, 2t_s, \ldots, Nt_s)$. Founded by the quadratic output estimation error, both the determined layouts for linear dynamic system $H$ and nonlinear function $g$ are correspondingly represented by notations $\overline{H}$ and $\overline{g}$, with $\overline{z}(t) = \overline{H}(p)\overline{g}(u(t))$. Fabricating a robust continuous-time Hammerstein model resulted in the formulation of the problem as **Problem 2.1**:

**Problem 2.1.** Retrieve $\overline{H}$ and $\overline{g}$ for the continuous-time Hammerstein model from Fig. 1 to generate a minimized $J(\overline{H}, \overline{g})$ with respect to the input and output data of $(u(t), z'(t))(0, t_s, 2t_s, \ldots, Nt_s)$.

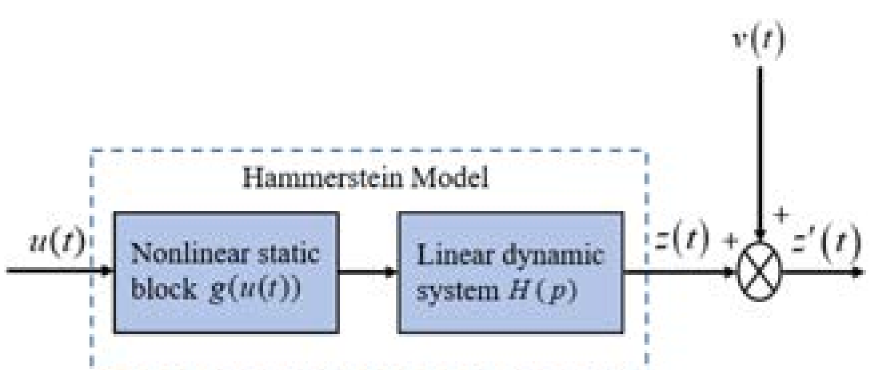


**Fig. 1.** The system diagram of continuous-time Hammerstein for the SISO model.

## 4. Identification method using normalized SPSA (N-SPSA)

An approach to resolve **Problem 2.1** is hereby given. Following an initial evaluation of the conventional SPSA-based method from (James C Spall, 1992), the revised SPSA-based method has been detailed, as subsequently manifested within the N-SPSA algorithm. The procedure for implementing the N-SPSA technique to identify a continuous-time Hammerstein system is outlined.

### 4.1. Review of the conventional SPSA algorithm

Consider both the objective function and design variable as $f:\Re^n\rightarrow\Re$ and $\theta\in\Re^n$, respectively. The expression for the generalized optimization problem is then written as:

$$\min_{\theta\in\Re^n} f(\theta). \tag{5}$$

The conventional SPSA algorithm updates Notation $\theta$ from the optimization problem shall be iteratively revised through implementation of the conventional SPSA-based method by operationalization of the updated equation:

$$\theta(k+1)=\theta(k)-a(k)\eta(\theta(k),\Delta(k)) \tag{6}$$

where $\theta(k)\in\Re^n$ symbolises the design variable at $k$ iteration and the gain sequence are correspondingly represented by notations $\theta(k)\in\Re^n$ and $a(k)\in\Re_+$, with its gradient approximation of $\eta(\theta(k),\Delta(k))\in\Re^n$ being further written as:

$$\eta(\theta(k),\Delta(k))=\begin{bmatrix}\dfrac{f(\theta(k)+c(k)\Delta(k))-f(\theta(k)-c(k)\Delta(k))}{2c(k)\Delta_1(k)}\\ \dfrac{f(\theta(k)+c(k)\Delta(k))-f(\theta(k)-c(k)\Delta(k))}{2c(k)\Delta_2(k)}\\ \vdots\\ \dfrac{f(\theta(k)+c(k)\Delta(k))-f(\theta(k)-c(k)\Delta(k))}{2c(k)\Delta_n(k)}\end{bmatrix}. \tag{7}$$

As such, Eq. (7) specified an additional gain sequence of $c(k)\in\Re_+$, with both randomly perturbated vector and the corresponding $i$ th element being independently denoted by notations $\Delta(k)\in\Re^n$ and $\Delta_i(k)\in\Re$. A simplified explanation is concerted on the symbolising of the vector $(k)$ 's $i$-th element. Both expressions of $a(k)=a/(k+1+A)^\alpha$ and $c(k)=c/(k+1)^\gamma$reflectively describe the respective gain sequences of $a(k)$ and $c(k)$ which are the current approach that purposely anticipates the close equivalence between both $\eta(\theta(k),\Delta(k))\in\Re^n$ and gradient of objective function $f$, i.e. $\frac{\partial f}{\partial\theta}(\theta(k))$, in which Eq. (6) prevails as a stochastic steepest descent.

The evaluation of performance conducted in (Tanaka et al., 2015) revealed an even greater likelihood of convergence instability arising from the conventional SPSA technique. Such deficiency is attributable to an excessively inflated value as excessively propelled by the gradient approximation vector from Eq. (7). The challenge is validated by using a simplified numerical example to illustrate unstable convergence via conventional SPSA technique control. Consider the objective function:

$$f(\theta)=\left((\theta-1)^T(\theta-1)\right)^3 \tag{8}$$

where $\theta_i=1$ denotes the global minimum point for $i=1,2,\ldots,10$, $a(k)=0.05/(k+200)^{0.602}$ is proposedly set, with $c(k)=0.01/(k+1)^{0.101}$ and $\Delta(k)$ being further attained through the random Bernoulli vector for $\theta_i(0)=0$ at $i=1,2,\ldots,10$. The results in Fig. 2 exhibit the responded convergence for the objective function of the conventional SPSA-based method succeeding the 30th iteration, without apparent acquisition of the global minimum point ensuing operation of its maximum value. The recorded outcomes verified the technique's failure to guarantee a stable convergence throughout conducted iterations in entirety. Such dissatisfactory performance initiated subsequent algorithmic betterment to the conventional SPSA-based approach.

### 4.2. Improved SPSA algorithm using normalized function

SPSA's limited proficiency for stable convergence is overcome by algorithmic integration of normalized function. Tackling the overreaching value of $k=\infty$the gradient approximation vector $\eta(\theta(k),\Delta(k))$ sees the appropriated restraint through the normalized function across conducted iterations in entirety. This is achievable by primarily delineating $f(\theta^+)$ and $f(\theta^-)$ to the respective functions of $f(\theta(k)+c(k)\Delta(k))$ in simplifying the expressed equation. A performed revision to the original vector from Eq. (6) produced: $\theta(k+1)=\theta(k)-a(k)\tilde{\eta}(\theta(k),\Delta(k))$ (9) where

$$\tilde{\eta}(\theta(k),\Delta(k))=\begin{bmatrix}\dfrac{\hbar(\tilde{f}(\theta^+),\tilde{f}(\theta^-))}{2c(k)\Delta_1(k)}\\ \dfrac{\hbar(\tilde{f}(\theta^+),\tilde{f}(\theta^-))}{2c(k)\Delta_2(k)}\\ \vdots\\ \dfrac{\hbar(\tilde{f}(\theta^+),\tilde{f}(\theta^-))}{2c(k)\Delta_n(k)}\end{bmatrix}. \tag{10}$$

Notably, $\hbar(\tilde{f}(\theta^+),\tilde{f}(\theta^-))$ from Eq. (10) is a contemporary function with the expression of:

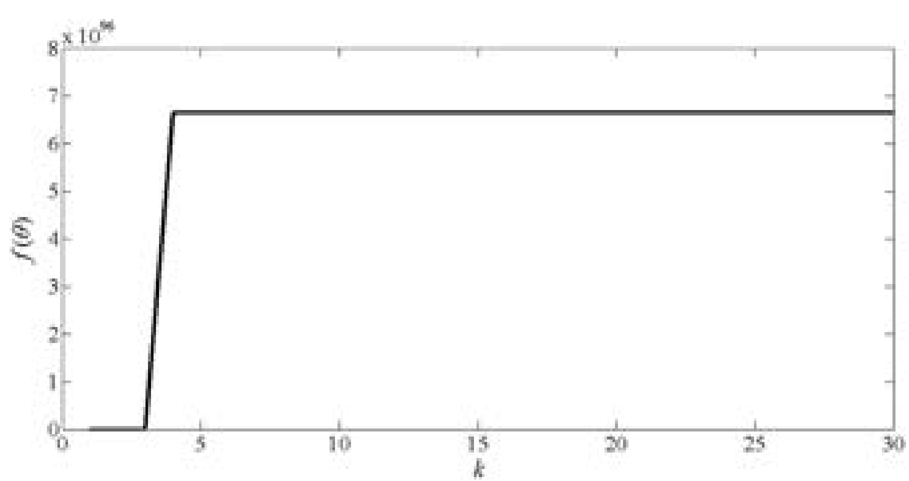


**Fig. 2.** The $f(\theta)$convergence response of the conventional SPSA.

$$\hbar(\widetilde{f}(\theta^+),\widetilde{f}(\theta^-)) = \begin{cases} 1 & \text{if } \widetilde{f}(\theta^+) = \widetilde{f}(\theta^-), \\ \widetilde{f}(\theta^+) - \widetilde{f}(\theta^-) & \text{if } \widetilde{f}(\theta^+) \neq \widetilde{f}(\theta^-), \end{cases} \tag{11}$$

where $\widetilde{f}(\theta^{\pm})$ represents a normalized objective function with the expression of:

$$\widetilde{f}(\theta^{\pm}) = \frac{f(\theta^{\pm})}{\max\{f(\theta^+), f(\theta^-)\}}. \tag{12}$$

Based on the modifications above, the large value produced by either one or both measurements of the objective function can be avoided prior to the performance of gradient approximation by adopting the normalized calculation in Eq. (12). Following this, the function in Eq. (11) is introduced to avoid zero perturbation to the updated design variable when an identical value is produced by both measurements of the objective function. Hence, it will result in the algorithm's continuous search for an optimum design variable. Ultimately, gradient approximation in Eq. (10) will still be performed by the enhanced algorithm off measurements of the normalized objective function. The detailed procedure for the N-SPSA is presented in Algorithm 4.2 as follows:

Algorithm 4.2. Pseudocode of the N-SPSA algorithm.

Initialize values $(a, A, \alpha, c, \gamma, \theta, k_{max}(\ ))$
For $k = 1$to $k_{max}$do
  Simulate $\Delta_n(k) \sim \{Bernoulli(-1,+1)\}^n$for $k = 1,\ldots,k_{max}$
  $a(k) = \dfrac{a}{(k+1+A)^{\alpha}}$
  $c(k) = \dfrac{c}{(k+1)^{\gamma}}$
  $f(\theta^{\pm}) = \theta(k) \pm c(k)\Delta(k)$
  $\widetilde{f}(\theta^{\pm}) = \dfrac{f(\theta^{\pm})}{\max\{f(\theta^+), f(\theta^-)\}}$
  $\hbar(\widetilde{f}(\theta^+),\widetilde{f}(\theta^-)) = \widetilde{f}(\theta^+) - \widetilde{f}(\theta^-)$
if $\hbar(\widetilde{f}(\theta^+),\widetilde{f}(\theta^-)) = 0$
  $\hbar(\widetilde{f}(\theta^+),\widetilde{f}(\theta^-)) = 1$
  else
  end if
  $\widetilde{\eta}(\theta(k),\Delta(k)) = \left(\dfrac{\hbar(\widetilde{f}(\theta^+),\widetilde{f}(\theta^-))}{2c(k)\Delta_n(k)}\right)$
  $\theta(k+1) = \theta(k) - a(k)\widetilde{\eta}(\theta(k),\Delta(k))$
end for
end procedure

Regarding time complexity of N-SPSA, we consider the non-trivial steps in N-SPSA as presented in **Algorithm 4.2** which includes Eq. (1) updating design parameter and Eq. (2) objective function measurements. To update the design parameter, we multiply the constant $a(k)$ and $\widetilde{\eta}$ which requires $p$ multiplications. The complexity of the normalized objective function measurement is clearly equivalent to the complexity of the objective function measurement even if it is perturbed with noise. Thus, for a given dataset, the algorithmic complexity of the N-SPSA is linear with the complexity of the underlying identification problem used in the evaluation of the fitness function in Eq. (4), which is based on the error of the identified model output and the actual output data of the experiment. Then, for the maximum iterations $k_{max}$ and dimensionality of the problem $p$, the time complexity of the NL-SPSA can be expressed as $O(k_{\max} \times p)$.

**Algorithm 4.2** was consecutively employed to resolve the arithmetical objective function from Eq. (8) towards efficacy appraisal of the N-SPSA-based method where the introduced approach from Eq. (9) was hereby implemented to achieve an unchanged setup of the previously explained conventional SPSA-based method with the exception $a(k) = 1.2/(k+200)^{0.602}$. The generated outcomes in Fig. 3 conclusively exhibited stable convergence from the proposed N-SPSA in **Algorithm 4.2** for the resolution of objective function within Eq. (8). It then laid far-reaching prospects for the integration of normalized function into the conventional SPSA to overcome the initially prevailed challenge of convergence instability.

### 4.3. Normalized SPSA (N-SPSA) algorithm for continuous-time Hammerstein model identification

The implementation of **Algorithm 4.2** in estimating the continuous-time Hammerstein model is described. The issue is primarily addressed through the re-expressing of fitness function from Eq. (4) as follows:

$$J(\beta) = \sum_{j=0}^{N} (z'(jt_s) - \overline{z}(jt_s))^2 \tag{13}$$

for the design variable

$$\beta = [\overline{b}_0, \overline{b}_1, \ldots, \overline{b}_{l-1}, \overline{a}_0, \overline{a}_1, \ldots, \overline{a}_{m-1}, \overline{\delta}_0, \overline{\delta}_1, \ldots, \overline{\delta}_M] \in \Re^c \tag{14}$$

where $c = l + m + M + 1$, with $\beta$ being a formerly identified fixed design parameter. Magnitudes of both $z'(jt_s)$ and $\overline{z}(jt_s)$ are further gauged using the predisposed action plan to acquire the required value of $J(\beta)$. It involves the initial fabrication of input signal $(u(t), z'(t))(t = 0, t_s, 2t_s, \ldots\ldots, Nt_s)$ prior the computation of

$$\overline{z}(t) = \frac{\overline{b}_l q^l + \overline{b}_{l-1} q^{l-1} + \ldots + \overline{b}_0}{q^m + \overline{a}_{m-1} q^{m-1} + \ldots + \overline{a}_0} \overline{g}(u(t)) \tag{15}$$

as comparably included within the continuous-time signal. A fixed sampling interval of $j = 0, 1, 2, \ldots, N$, $\overline{z}(jt_s)$ is generated as the sample $\overline{z}(t)$ before subsequent operationalization of N-SPSA for the identification of the continuous-time Hammerstein model. The systematic procedure of

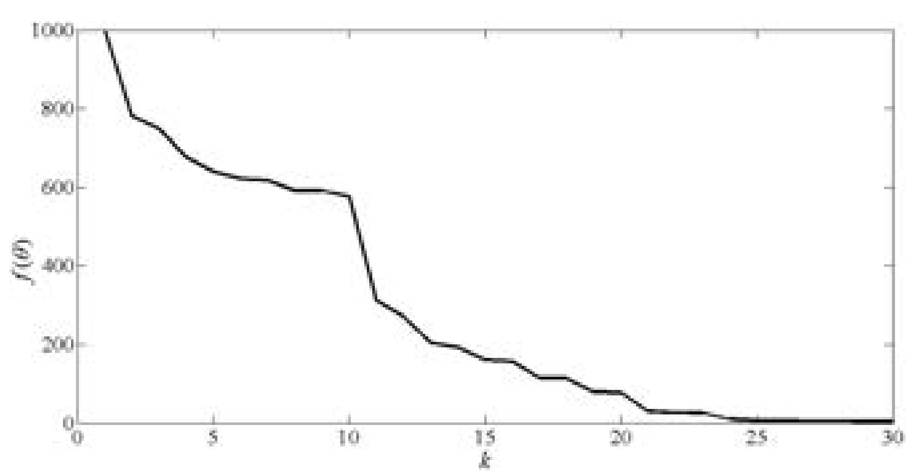


**Fig. 3.** The $f(\theta)$convergence response of the N-SPSA.

the current undertaking is summarised by:

**Step 1:** The value of maximum iterations $k_{max}$ for the N-SPSA-based method from Eq. (9) is identified. The value of $\theta(0)$ is then initialized at $\beta_i = \theta_i(i = 1, 2, \ldots, c)$.

**Step 2: Algorithm 4.2** for the N-SPSA-based method is operated towards the objective function of $J(\beta) = f(\theta)$.

**Step 3:** $\theta^* := \theta(k_{max}())$ is acquired upon achieving iteration $k_{max}$, with output $\beta^* := [\theta^*{}_1, \theta^*{}_2, \ldots, \theta^*{}_c]$ as the solution to **Problem 2.1**.

## 5. Results and discussion

The effectiveness of the N-SPSA-based method in estimating the continuous-time Hammerstein system is hereby justified. Real-time experimentation data have been assumed to identify both the TRS and the EMPS by implementing the N-SPSA-based method. These systems were purposefully chosen for their ability to accurately replicate intricate real-world dynamics, ensuring a comprehensive assessment of the N-SPSA-based method's efficiency in handling practical scenarios. Both systems have been successfully implemented (Brunot et al., 2015; Alexandre Janot et al., 2017; Jui & Ahmad, 2021; Mok & Ahmad, 2024), where the system's nonlinearity is represented by the friction phenomenon in both systems. In the TRS system, nonlinearity stems from the friction of the rotor shaft during vertical motion. While, in the EMPS, nonlinearity arises from Coulomb friction from the ball screw drive's positioning unit. A comparative analysis was undertaken to examine the N-SPSA-based method and other algorithmic approaches, including the conventional SPSA (James C Spall, 1992), NL-SPSA (Ahmad et al., 2016), and AMVO-SCA-based (Jui & Ahmad, 2021) methods. The selection of those algorithms allows for a comparative assessment between single-agent and multi-agent optimization methods as well as existing variants of SPSA in identifying Hammerstein systems. The aim is to explore how each approach addresses significant challenges in Hammerstein system identification, encompassing constraints related to a significant range of design parameters in the continuous-time model, and the computational time evaluated based on the number of function evaluations.

The performance of the investigated approaches was measured in accordance with a series of pre-determined criteria.

i. The analysis of the obtained response in the best fitness function of the identified TRS and EMPS models across 25 independent trials was based on both time and frequency domains.
ii. Recorded mean, best, worst, and standard deviation (Std.) values were utilized to appraise the statistical outcomes of fitness functions across 25 independent trials for the N-SPSA, the original SPSA (James C Spall, 1992), the NL-SPSA (Ahmad et al., 2016), and the AMVO-SCA (Jui & Ahmad, 2021) methods.
iii. The NFE was evaluated for 25 independent trials.
iv. Wilcoxon's rank test (Jui & Ahmad, 2021) was used as a non-parametric statistical test with a 5 % significance level to evaluate statistical differences between examined algorithms. The mean of the fitness function was computed across 25 independent trials, and the significance level was determined by analyzing the simulated results and determining the values for and employing two distinct algorithms. The performance robustness of analyzed algorithms would vary in the event, but it would remain constant if or not. The performance robustness of the examined algorithms would differ in the case where $p = 0.05$ or $h = 1$, and similar in the case where $p > 0.05$ or $h = 0$.

### 5.1. Twin-rotor system (TRS)

This section specifies modeling the continuous-time Hammerstein system in the fabrication of a TRS through the proposed employment of N-SPSA. An experimental laboratory-sized helicopter structure with fundamental traits, including coupling and a high level of nonlinearity, was adopted by this study. The structure known as the TRS identifies a complicated hovering craft that necessitates intricate modeling, handling, and operation, similar to a real-time helicopter that experiences parametric alterations in response to shifts in flight conditions. As a result, the importance of system identification for improved modeling of aerial transportation in the face of varying flight conditions is practically acknowledged.

The simulated settings of the TRS comprised the installation of the main and tail rotors with a mechanical capacity for unhindered rotations across vertical and horizontal planes. The rotors pivot on the structure's base, as they were installed on both ends of the horizontal beam. The beam can be modified by manipulating the input voltage to administer both rotors' rotational speed, with its rotation and maneuver moving towards the ends of spherical surfaces, further enabled by the joint. A pendulum was also linked to the beam to ensure steady angular motions. A TRS with a computerized interface has been developed, as illustrated in Fig. 4 (Toha et al., 2012). The blades for the primary and tail rotors are observably appropriated to the rotations around both yaw and pitch axes to enable the system's vertical and horizontal maneuvers. However, such flexible rotations would result in vibrations amid commanded motions in light of an imbalanced mass distribution.

Regarding the direct causation between the input via the vertical channel and the TRS's vibrational motions, primarily encountered at the pitch angle, the vertical channel defines the system's output. Its input then adheres to an arbitrary signal of 1 V at a sample interval of 0.1 s. The system's vertical channel is approached by gathering 600 s in simulated input-output data as the statistical basis for its modeling.

Fig. 5 systemizes the block diagram of the continuous-time Hammerstein system that is used to validate the TRS model, with the estimated output, as well as the recorded output and input through modular experimentation, being separately represented by notations $\overline{y}(t)$, $y(t)$, and $u(t)$, respectively. The responses for both the input signal $u(t)$ and vertical channel output $y(t)$ are then independently portrayed in Figs. 6 and 7 under presumed conditions where the measurement noise has been accounted for by the vertical channel output.

The experimentations were set to investigate both linear and nonlinear subsystems as configured by the description provided (Jui & Ahmad, 2021). The nonlinear subsystem is crucial in ascertaining nonlinear friction via the rotor shaft amid vertical motion. The currently investigated system's nonlinear and linear modules were hereby modeled in accordance with the second-order continuous-time transfer function and the tangent hyperbolic function, respectively. They are then correspondingly expressed by:

$$\overline{H}(p) = \frac{p + \overline{b}_0}{p^2 + \overline{a}_1 p + \overline{a}_0} \tag{16}$$

$$\overline{g}(u(t)) = \overline{\delta}_0 \tanh(\overline{\delta}_1 u(t)) \tag{17}$$

The initial design variables have been notably shortlisted through several preliminary experimentations and primary investigations (Jui & Ahmad, 2021). Following the illustrated information in Table 1, a total of five initially unknown design variables for the TRS's nonlinear and linear parameters are ascertained under the coefficient settings specified for the conventional SPSA, the NL-SPSA, and the N-SPSA from Table 2.

Table 3 outlined the most statistically preferred objective functions for the examined SPSA, NL-SPSA, AMVO-SCA, and N-SPSA-based methods across 25 independent trials. The conventional SPSA-based method has difficulties recognizing the Hammerstein-modeled TRS due to unstable convergence in the respective objective functions, leading to inconsistent results and higher variability. This instability highlights SPSA's inherent challenge in achieving consistent and reliable parameter optimization for complex nonlinear systems.

In contrast, integrated algorithmic approaches such as the N-SPSA and the NL-SPSA effectively mitigated these issues during successive

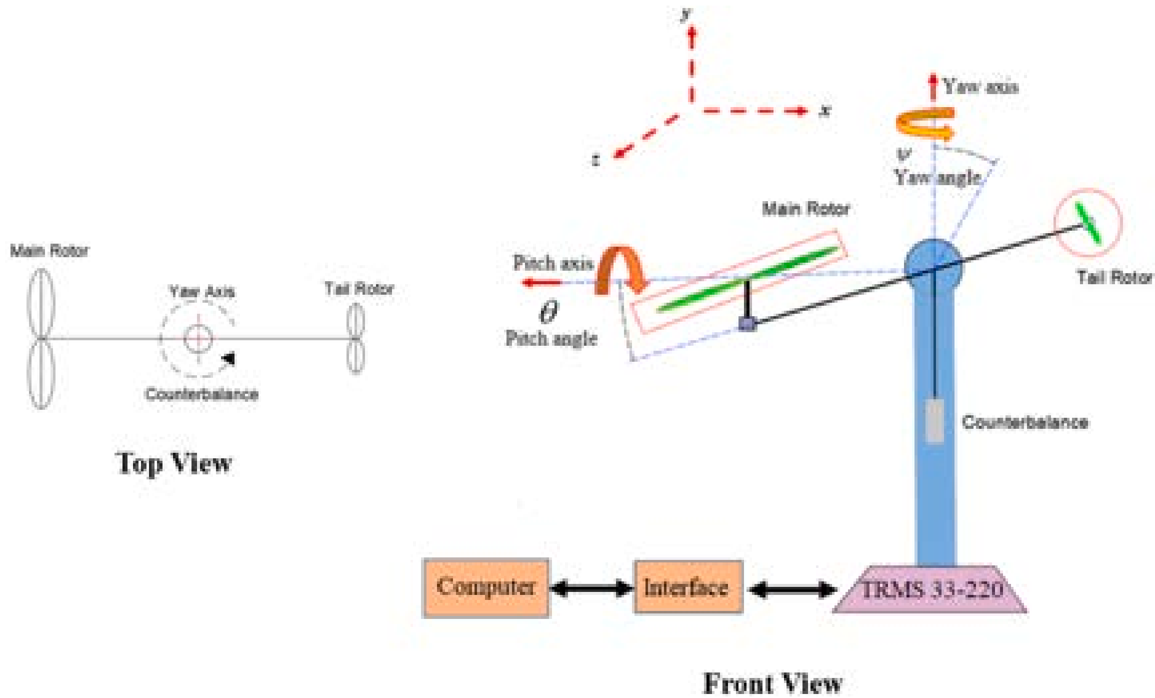


**Fig. 4.** The system diagram of the TRS (Toha et al., 2012).

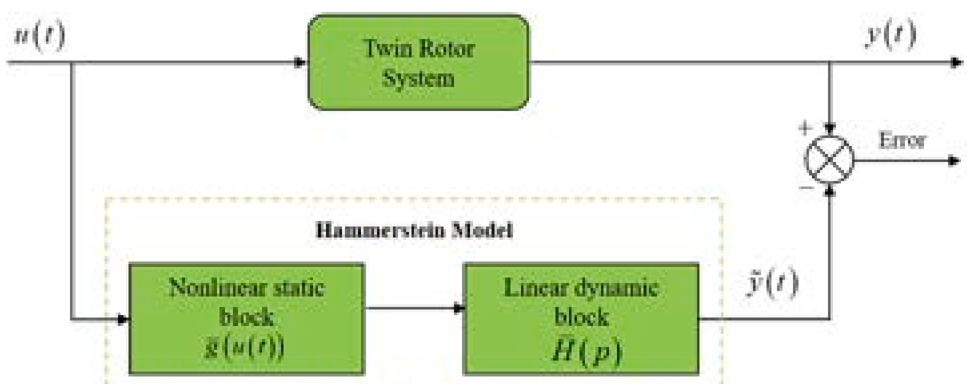


**Fig. 5.** Block diagram to validate the TRS model using the Hammerstein model.

model identifications. The N-SPSA, in particular, demonstrated the most consistent objective function measurements across trials, achieving the smallest standard deviation and the lowest mean value among all the methods. Specifically, the N-SPSA exhibited a 3.42 % improvement in mean objective function compared to the NL-SPSA and an 18.09 % improvement over the AMVO-SCA. The reductions in the mean highlighted the N-SPSA's superior reliability in successive model identifications. Additionally, the N-SPSA standard deviation had improved by 87.06 % compared to the NL-SPSA and an impressive 99.64 % compared to the AMVO-SCA, showcasing its robust ability to deliver accurate results consistently. While the AMVO-SCA achieved a marginally better best value on the objective function (by approximately 0.3 %), N-SPSA's overall consistency and reliability metrics were superior, making it a more competitive choice for Hammerstein system identification.

The NFE for the SPSA, the NL-SPSA, and the N-SPSA was consistently set at 2000, as shown in Table 3. Notwithstanding, the proposed N-SPSA-based method eclipsed the AMVO-SCA under a significantly reduced NFE condition, requiring only 2000 NFE compared to the AMVO-SCA's 5000 NFE. This represents a substantial reduction of 60 % in computational effort. This demonstrates the superiority of the N-SPSA-based approach over the AMVO-SCA-based approach in terms of objective function optimization at lower functional evaluations. With the proposed method demonstrating promising robustness across all examined alternatives, Table 4 details the best design variable values for each of the 25 included methods. Current findings revealed a significant disparity in the best value between the conventional SPSA and its integrated NL-SPSA, N-SPSA, and AMVO-SCA counterparts, attributable to convergence instability limitations.

Building on the significant reduction in NFE discussed previously, Figs. 8, 10, and 12 separately outline the findings for the TRS's vertical channel in terms of output and error responses, as well as power spectrum density, using each of the methods examined. Detailed dissimilarities of the generated results from the conventional SPSA, the NL-SPSA, the AMVO-SCA, and the N-SPSA-based methods are simultaneously observed through the independently magnified layouts of the output and error responses in Fig. 9 and Fig. 11. The TRS responses from the vertical channel, shown in Fig. 9, indicate that the implementation of the N-SPSA closely matches the system's actual signal, reflecting its ability to minimize deviations and achieve high fidelity.

In comparison, the responses from other methods, including the

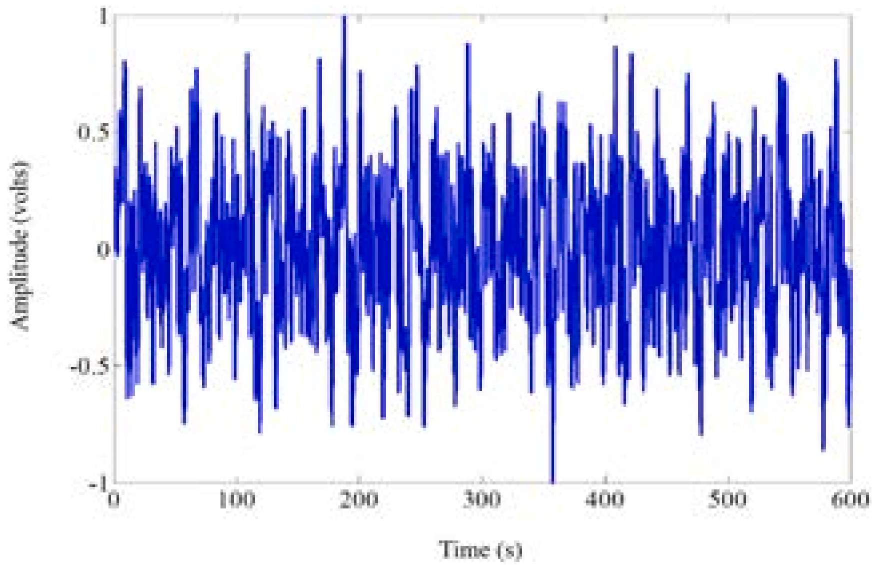


**Fig. 6.** Vertical input channel $u(t)$.

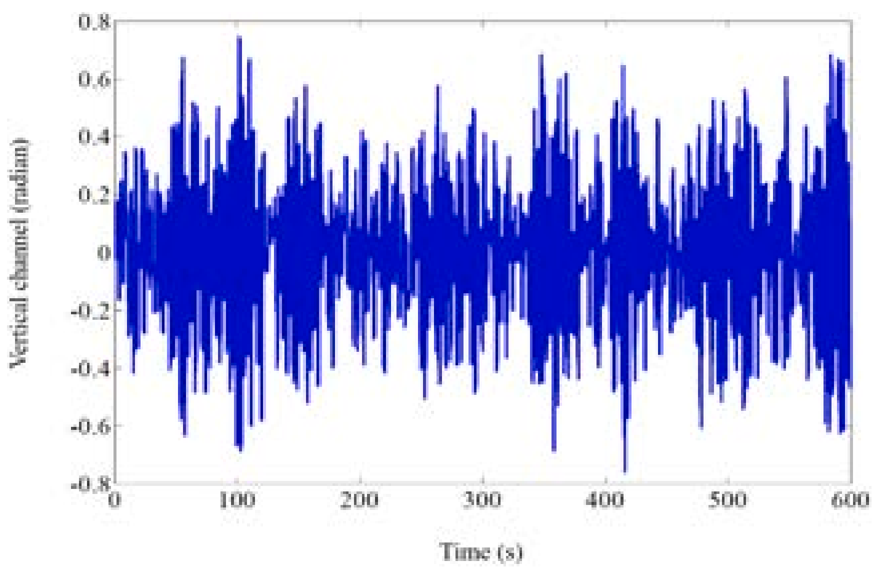


**Fig. 7.** Vertical output channel $y(t)$.

**Table 1**
Initial values for the TRS model.

| $\beta$ | Designed variables | $\theta(0)$ |
|---|---|---|
| $\beta_1$ | $b_0$ | $-2.0000$ |
| $\beta_2$ | $a_0$ | 0.0000 |
| $\beta_3$ | $a_1$ | 5.0000 |
| $\beta_4$ | $\delta_0$ | $-5.0000$ |
| $\beta_5$ | $\delta_1$ | 0.0000 |

**Table 2**
Coefficient of the SPSA algorithms for the TRS.

| SPSA | NL-SPSA | N-SPSA |
|---|---|---|
| $k_{max}$ | $k_{max}$ | $k_{max}$ |
| $a(k) = 0.02 / (k+10)^{0.9}$ | $a(k) = 800/(k+10)^{0.9}$ | $a(k) = 0.025/(k+11)^{0.3}$ |
| $c(k) = 0.1 / (k+1)^{1/6}$ | $c(k) = 0.1/(k+1)^{1/6}$ | $c(k) = 0.2/(k+1)^{1/3}$ |
| - | $sat_\delta = 0.01$ | - |

**Table 3**
The statistical analysis of the objective function and corresponding NFE for the SPSA, NL-SPSA, AMVO-SCA, and N-SPSA.

| Method | SPSA (James C Spall, 1992) | NL-SPSA (Ahmad et al., 2016) | AMVO-SCA (Jui & Ahmad, 2021) | N-SPSA |
|---|---|---|---|---|
| Mean | N/A | 185.3377 | 218.5541 | **179.0082** |
| Best | $1.4100\times10^{32}$ | 182.9412 | **177.9563** | 178.4851 |
| Worst | N/A | 189.2094 | 339.1072 | **179.3974** |
| Std. | N/A | 1.8982 | 69.0269 | **0.2457** |
| NFE | 2000 | 2000 | 5000 | **2000** |

SPSA, the NL-SPSA, and the AMVO-SCA, also aligned with the actual signal but showed slightly higher deviations, emphasizing N-SPSA's superior accuracy and stability in system identification. These findings are further supported in Fig. 10, which illustrates that the proposed N-SPSA method produced significantly lower error compared to both the conventional SPSA and the NL-SPSA approaches. Furthermore, the N-SPSA demonstrated a performance level comparable to the AMVO-SCA-

**Table 4**
The best-identified value for design variables of the SPSA, NL-SPSA, AMVO-SCA, and N-SPSA.

| | Design variables | SPSA (James C Spall, 1992) | NL-SPSA (Ahmad et al., 2016) | AMVO-SCA (Jui & Ahmad, 2021) | N-SPSA |
|---|---|---|---|---|---|
| $\theta_1^*$ | $b_0$ | $-2.3635\times10^{14}$ | $-1.9500$ | $-1.9078$ | 1.8160 |
| $\theta_2^*$ | $a_0$ | $2.3635\times10^{14}$ | 0.1100 | 4.7607 | 0.1180 |
| $\theta_3^*$ | $a_1$ | $2.3635\times10^{14}$ | 4.7500 | 0.1085 | 4.7681 |
| $\theta_4^*$ | $\delta_0$ | $2.3635\times10^{14}$ | $-1.1500$ | $-9.8045$ | $-4.7132$ |
| $\theta_5^*$ | $\delta_1$ | $-2.3635\times10^{14}$ | 0.4900 | 0.0574 | 0.1229 |

based approach but achieved this with 60 % fewer functional evaluations, as previously discussed, demonstrating its potential for more accurate and reliable system identification in TRS applications. A prominent resonance mode of 0.35 Hz exposed through the actual power-spectral density (PSD) were successively determined by the N-SPSA-based approach alongside the comparable efficacy of the other examined methods. These collective findings essentially validated the N-SPSA's capacity to address the challenges of achieving accurate system identification with fewer computational resources, aligning with the results demonstrated in the Hammerstein-modeled TRS simulation. (Jui & Ahmad, 2021).

Generated objective functions for the conventional SPSA, the NL-SPSA, and the N-SPSA were sequentially appraised using Wilcoxon's rank-sum test criteria. However, the unaltered SPSA-based method was excluded from this analysis due to its inherent constraint of convergence instability, which rendered its results inconsistent and unreliable. Consequently, the evaluation focused solely on the NL-SPSA and N-SPSA outcomes. The results demonstrated a $p$-value $5.08\times10^{-8}$ under a significance benchmark of 0.05, with a corresponding $h$-value of 1 for the proposed N-SPSA-based approach. These results underscore the statistically significant superiority of the N-SPSA-based method over the NL-SPSA-based approach in identifying the TRS. By producing a more robust and accurate objective function, the N-SPSA method effectively overcame the convergence instability inherent in traditional SPSA while providing improved system identification precision. These findings

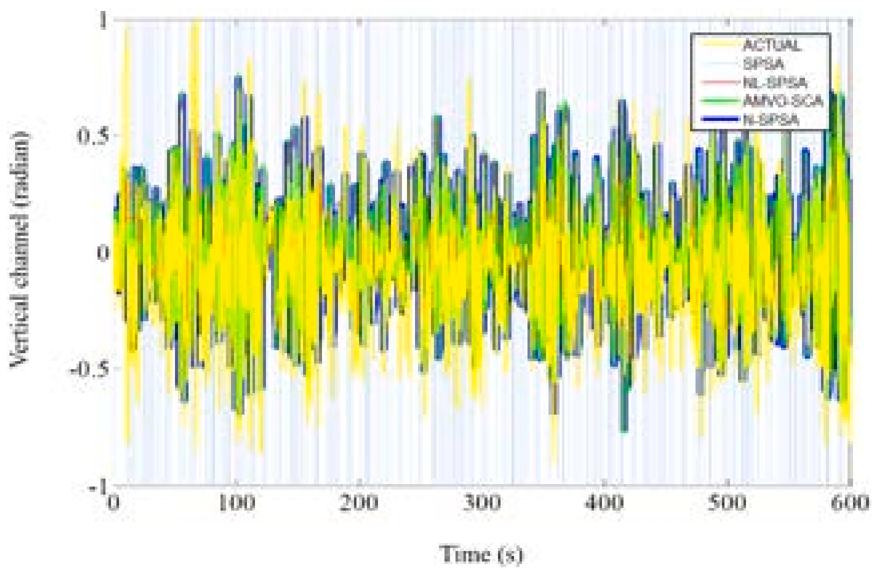


**Fig. 8.** Identified vertical output channel of the TRS.

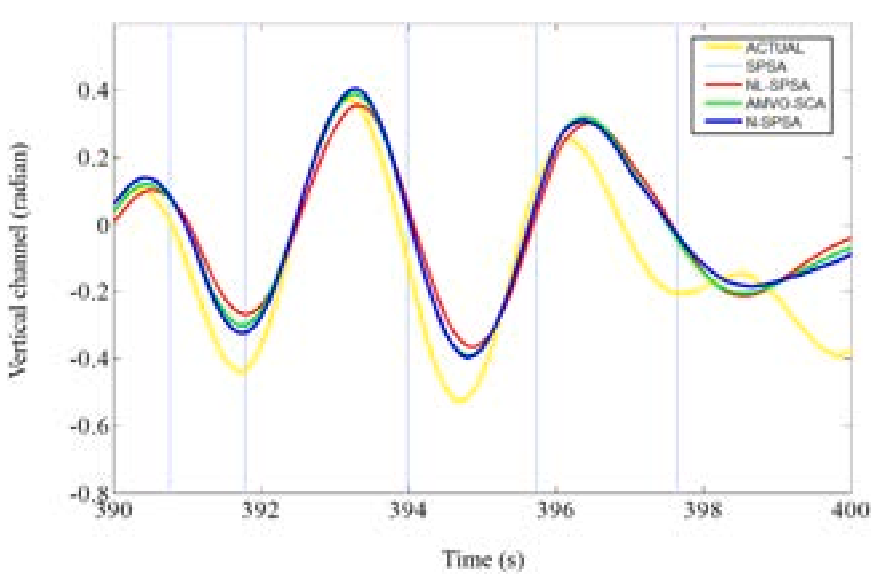


**Fig. 9.** Zoomed-in view of the output responses identified in Fig. 8.

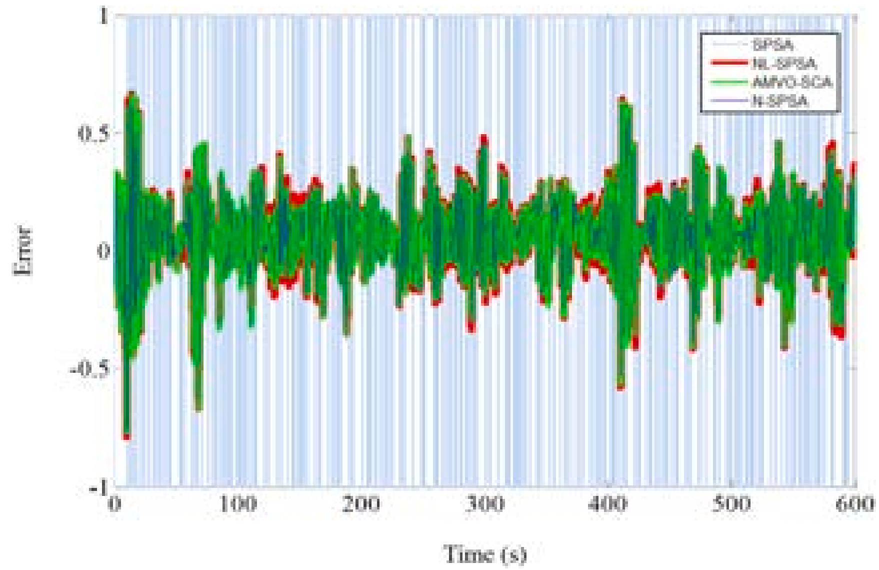


**Fig. 10.** TRS error responses.

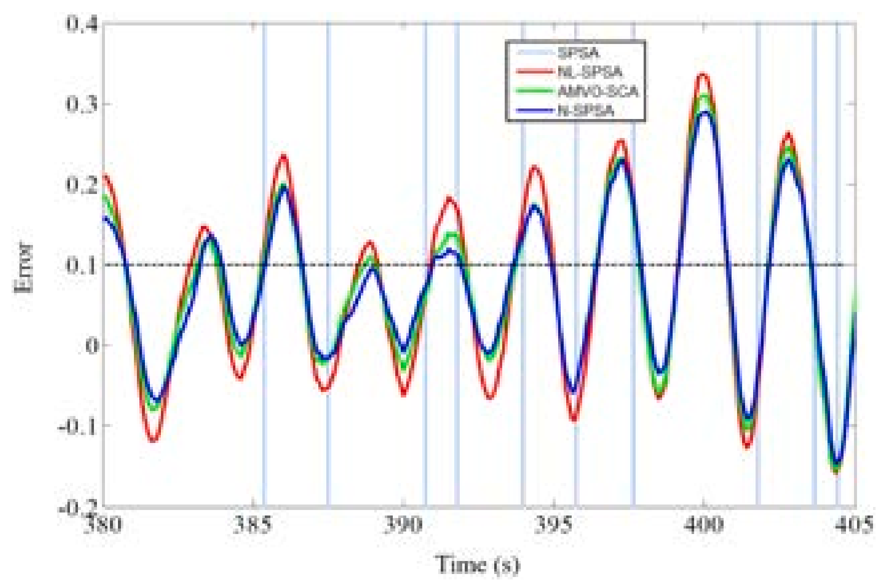


**Fig. 11.** Zoomed-in view of Fig. 10 corresponding to the error responses.

further validate the reliability and efficiency of the N-SPSA as a competitive alternative for optimizing complex nonlinear systems like the TRS.

### 5.2. Electro-mechanical positioning system (EMPS)

The current section evaluates the effectiveness of the N-SPSA-based method in identifying an EMPS by adopting continuous-time Hammerstein modeling. A nominally configured drive structure employed within the prismatic joint in the robotic and mechanical applications is depicted in Fig. 13, with the primary inclusion of a controller and a DC motor under installation of a 12,500-counts-per-revolution encoder, observable via its left structure. The manipulated application is controlled by a star high-precision, low-friction ball screw coupled to a DC motor, with an additional encoder mounted on the ball screw's outer edge for disposition locational measurement. As the object for positional measurement, a load in translation located in the middle of the EMPS with an affixed accelerometer is outfitted. Due to the inapplicability of numerical data, recorded by the encoder via the edge of the ball screw and the accelerometer, input and output data were utilized to assure data standardization and periodicity by employing the dSPACE digital control system. (A Janot et al., 2019). Input and output data for the EMPS analysis were sampled at a rate of 0.001 s per 12 s. Notably, the processing aspect was not evaluated, suggesting that the data involved may be in an unprocessed format. Fig. 14(a)–14(b), depict representations of the input data based on force and the output data based on position, respectively. Fig. 15 illustrates the block diagram from validating the EMPS's estimated model using the continuous-time Hammerstein model as its structural reference.

The linear and nonlinear elements of the EMPS were directly adopted (A Janot et al., 2019). The mathematical representations of both linear and nonlinear subsystems are expressed through the following formulas:

$$\overline{H}(p) = \frac{1}{p^2 + \overline{a}_1 p} \tag{18}$$

$$\overline{g}(u(t)) = \overline{\delta}_0 u(t) + \overline{\delta}_1 sign(u(t)) + \overline{\delta}_2 \tag{19}$$

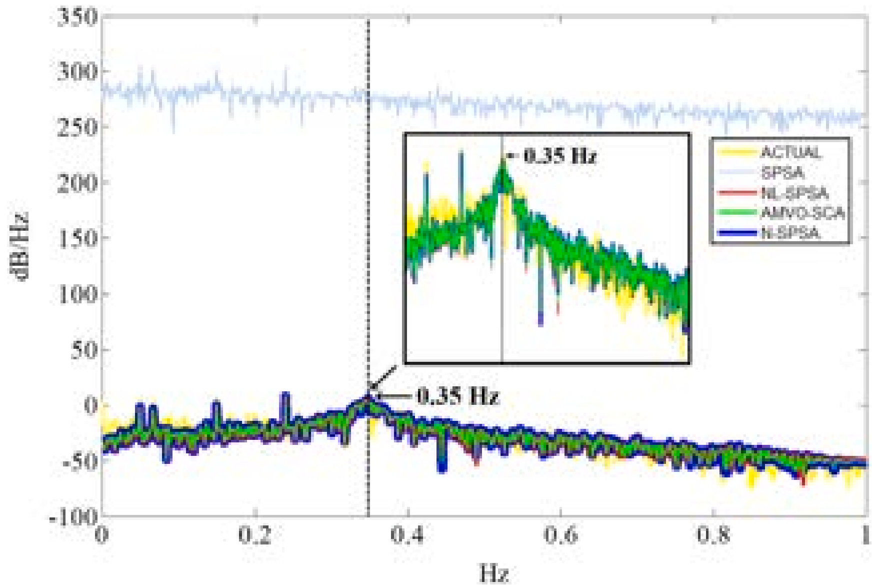


**Fig. 12.** Power spectrum density of the vertical channel.

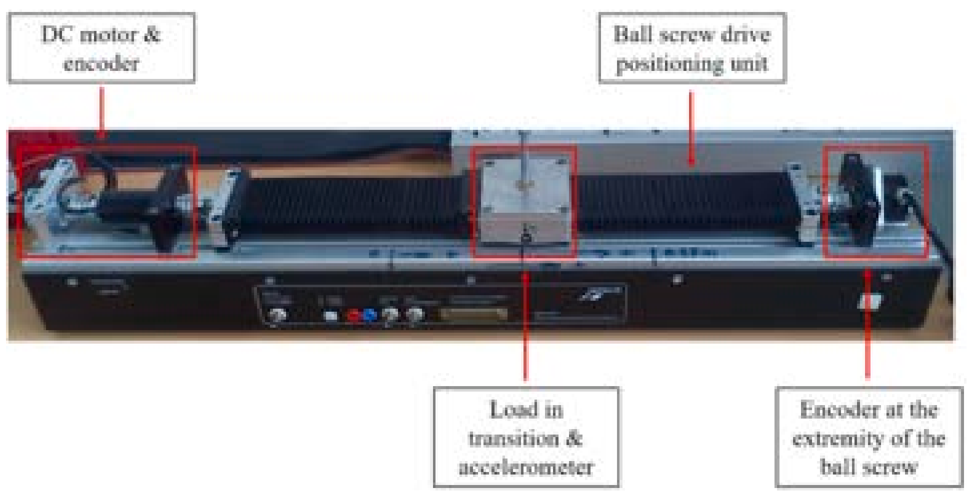


**Fig. 13.** Prototype of the EMPS. (A Janot et al., 2019).

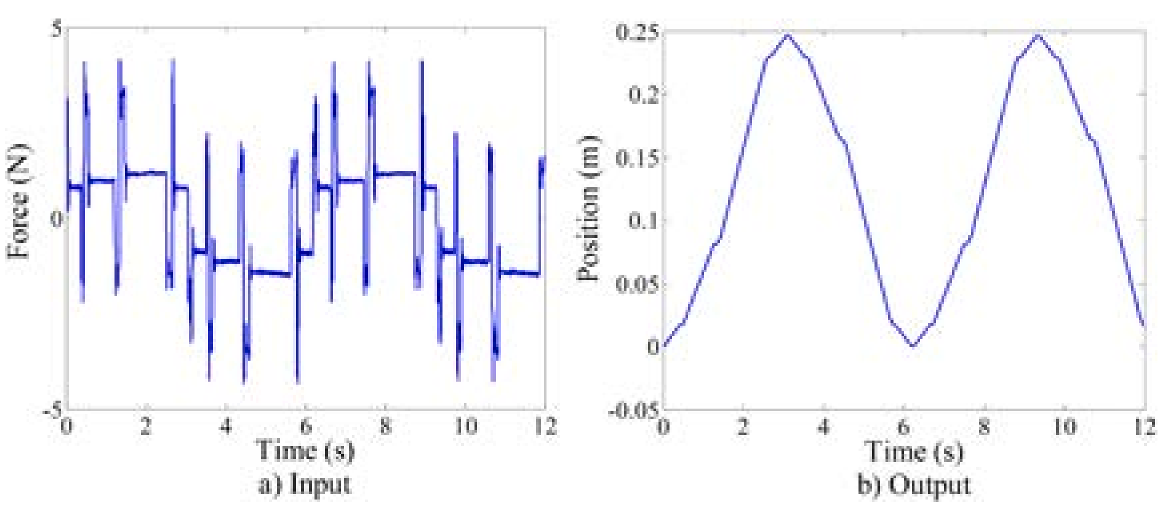


**Fig. 14.** Input and output signals of the EMPS.

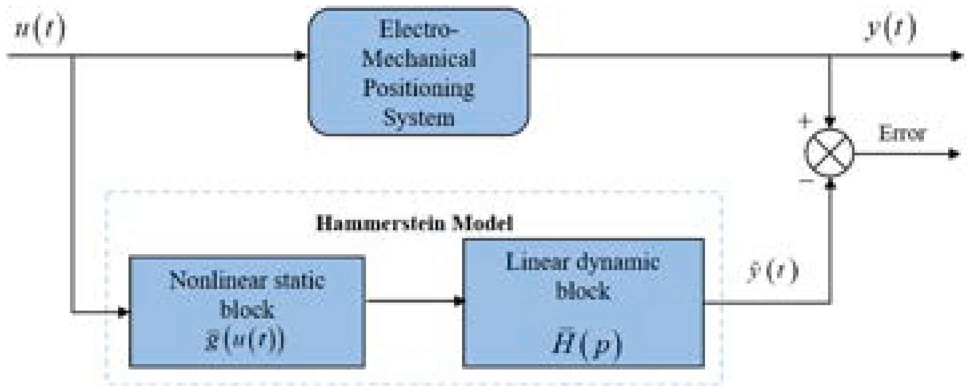


**Fig. 15.** Block diagram to verify the EMPS model with the Hammerstein model.

The second-order transfer function in Eq. (18) represents the linear subsystem of the EMPS system. From Eq. (19), the nonlinear subsystem is derived to account for the effects of Coulomb friction and offset. The proposed N-SPSA-based method aims to optimize four unknown design variables based on this Hammerstein model. Primary design variables centering on nonlinear and linear parameters for the EMPS are outlined in Table 5, while coefficient settings corresponding to the conventional SPSA, the NL-SPSA, and the N-SPSA-based methods are tabulated in Table 6. These initial design variables has been selected based on extensive preliminary experiments and an initial study conducted within the reference (A Janot et al., 2019). To assess the statistical performance, 25 independent runs were conducted to evaluate the N-SPSA--based method in comparison with the other methods.

Statistical findings of the objective function across separate trials for conventional SPSA, NL-SPSA, AMVO-SCA, and N-SPSA-based methods are presented in Table 7. The conventional SPSA-based method struggled to reliably identify the EMPS due to inconsistent convergence behavior, resulting in highly variable and unreliable outcomes. This limitation highlights the inherent challenges of the SPSA in achieving appropriate parameter identification for nonlinear systems. Conversely, integrated approaches such as the N-SPSA and NL-SPSA effectively resolved these issues during successive trials. Among these, the N-SPSA demonstrated exceptional performance, achieving the lowest average value and the most accurate results across trials. Specifically, the N-SPSA improved the mean objective function by 71.19 % compared to the NL-SPSA and by 25.18 % compared to the AMVO-SCA, underscoring its ability to deliver both accuracy and consistency. Furthermore, the standard deviation for the N-SPSA has improved by 87.72 % compared to the NL-SPSA and by 52.88 % compared to the AMVO-SCA, confirming its reliability in managing complex models. While the AMVO-SCA achieved marginally better best values (approximately 1.54 %), the N-SPSA demonstrated superior overall effectiveness in modeling the EMPS, emphasizing its strengths across comprehensive performance metrics. The NFE for the SPSA, the NL-SPSA, and the N-SPSA was consistently maintained at 2500, as shown in Table 7. In contrast, the AMVO-SCA required a significantly higher computational effort, operating with 5000 NFE, double the threshold of the other methods. This 50 % reduction in computational effort highlights the efficiency of the N-SPSA, which achieved comparable or superior results while utilizing fewer resources. Such efficiency makes the N-SPSA an ideal choice for real-time applications where precision must be balanced with computational efforts. Table 8 provides further details on the best design parameter values obtained across 25 trials, highlighting that the N-SPSA consistently outperformed the SPSA, the NL-SPSA, and the AMVO-SCA in overall performance. These findings also emphasize the limitations of the SPSA in achieving stable convergence and reinforce the practicality of the N-SPSA as a robust and efficient solution for complex system modeling.

The responses for the time-domain position and its zoom-in views have been separately illustrated in Figs. 16–17, with obtained simulation outcomes on the responses of position error for the EMPS via respective optimization of the SPSA, the NL-SPSA, the AMVO-SCA, and the N-SPSA-based methods. The labeling in the current figures also denotes underlined specifications related to the EMPS experimentation. As observed in Fig. 17, the position output obtained from the N-SPSA-based method closely resembled the actual position recorded from the EMPS

**Table 5**
Initial design variables of the EMPS.

| $\beta$ | Designed variables | $\theta(0)$ |
|---|---|---|
| $\beta_1$ | $\alpha_1$ | −1.0000 |
| $\beta_2$ | $\delta_0$ | 0.5000 |
| $\beta_3$ | $\delta_1$ | −0.4000 |
| $\beta_4$ | $\delta_2$ | 0.0000 |

**Table 6**
Coefficients of the SPSA, NL-SPSA, and N-SPSA algorithms for the EMPS.

| SPSA | NL-SPSA | N-SPSA |
|---|---|---|
| $k_{max}$ | $k_{max}$ | $k_{max}$ |
| $a(k) = 2 \times 10^{-4}/(k+24)^{0.9}$ | $a(k) = 9 \times 10^{-4}/(k+24)^{0.9}$ | $a(k) = 6.6 \times 10^{-1}/(k+24)^{0.9}$ |
| $c(k) = 0.2/(k+1)^{1/3}$ | $c(k) = 0.2/(k+1)^{1/3}$ | $c(k) = 0.2/(k+1)^{1/3}$ |
| - | $sat_\delta = 0.1$ | - |

**Table 7**
The statistical analysis of the objective function and NFE for the SPSA, NL-SPSA, AMVO-SCA, and N-SPSA.

| Method | SPSA (James C Spall, 1992) | NL- SPSA (Ahmad et al., 2016) | AMVO-SCA (Jui & Ahmad, 2021) | N-SPSA |
|---|---|---|---|---|
| Mean | N/A | 1.8550 | 0.7151 | **0.5364** |
| Best | N/A | 0.3022 | **0.2103** | 0.2444 |
| Worst | N/A | 7.2260 | 1.6604 | **1.0023** |
| Std. | N/A | 1.8067 | 0.4704 | **0.2217** |
| NFE | 2500 | 2500 | 5000 | **2500** |

**Table 8**
The best value of design variables utilizing the SPSA, NL-SPSA, AMVO-SCA, and N-SPSA.

| | Design variables | SPSA (James C Spall, 1992) | NL-SPSA (Ahmad et al., 2016) | AMVO-SCA (Jui & Ahmad, 2021) | N-SPSA |
|---|---|---|---|---|---|
| $\theta_1^*$ | $\alpha_1$ | $-1.5662\times10^6$ | 3.1102 | 3.1626 | 3.2870 |
| $\theta_2^*$ | $\delta_0$ | $-1.5662\times10^6$ | 0.6361 | 0.5485 | 0.59130 |
| $\theta_3^*$ | $\delta_1$ | $1.5662\times10^6$ | −0.5352 | −0.4019 | −0.4448 |
| $\theta_4^*$ | $\delta_2$ | $-1.5662\times10^6$ | 0.0552 | 0.0457 | 0.0486 |

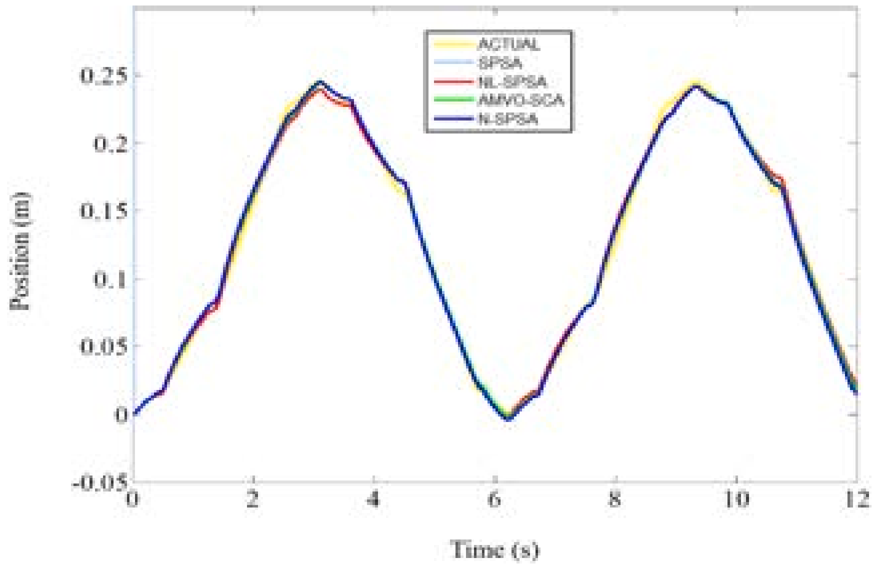


**Fig. 16.** Time domain position response (normal).

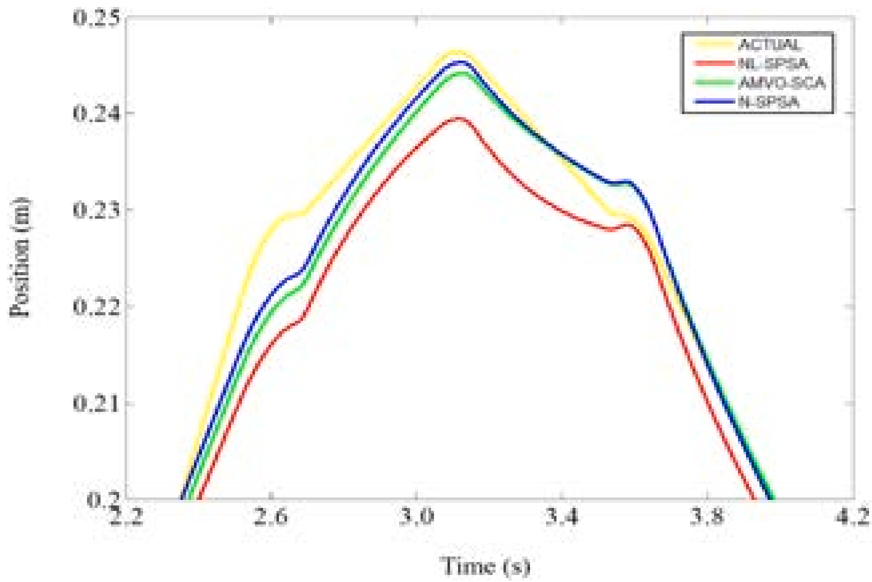


**Fig. 17.** Time domain position response (zoomed-in view of Fig. 16).

hardware, indicating its superior accuracy in capturing the system dynamics. This established the N-SPSA as a robust choice for system identification and control tasks. The AMVO-SCA approach also performed competitively, with deviations slightly larger than those of the N-SPSA. In contrast, both SPSA and NL-SPSA exhibited significant deviations from the actual position in the overall response (Fig. 16), particularly around the peaks, where they consistently produced lower values, indicating their inability to capture the system dynamics effectively. However, in the zoomed-in view (Fig. 17), NL-SPSA's deviation became even more pronounced, while SPSA was less dominant in this region, further highlighting its failure to accurately track the actual response. These findings were consistently corroborated by the results shown in Fig. 18, where the proposed N-SPSA-based method demonstrates significantly lower error than the conventional SPSA and the NL-SPSA methods, underscoring its ability to effectively minimize system errors. Additionally, the AMVO-SCA approach exhibited competitive performance, with error amplitudes slightly higher than those of the N-SPSA. In contrast, the NL-SPSA and SPSA produced significantly larger errors, with the SPSA exhibited the highest error amplitudes. These results confirmed the robustness of the N-SPSA in system identification tasks, consistently outperforming the other methods in accuracy and stability.

Additional efforts were made to differentiate the respective objective functions of the N-SPSA and the NL-SPSA-based methods through the implementation of Wilcoxon's rank-sum test. The conventional SPSA approach was excluded from the EMPS experimentation due to its prevailing instability which rendered its result inconsistent and unreliable. The analysis yielded a $p$-value of 0.0015 at a significance benchmark of 0.05, along with a corresponding $h$-value of 1, confirming the statistical superiority of the N-SPSA-based method over the NL-SPSA-based method. These findings demonstrate that the N-SPSA effectively resolves the instability and variability observed in the traditional SPSA while achieving greater precision in developing an accurate EMPS Hammerstein model. The robustness and reliability of the N-SPSA-based method were further validated across the majority of trials, solidifying its position as an efficient solution for nonlinear system identification.

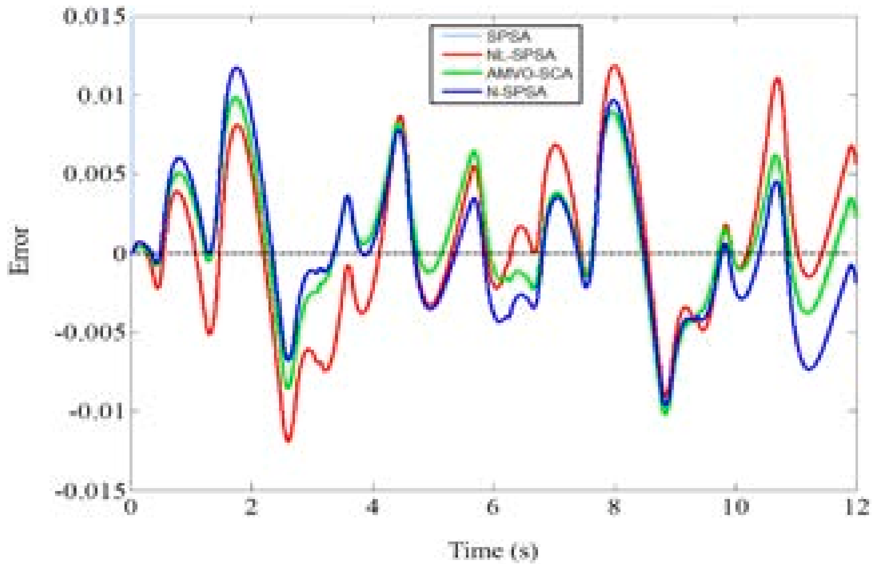


**Fig. 18.** Error responses of the EMPS.

## 6. Conclusion

A renewed algorithmic approach known as the N-SPSA is introduced to enhance the stability of the conventional SPSA approach. This novel strategy, achieved by controlling design variable updates through normalization, has demonstrated successful applications in determining continuous-time Hammerstein models. Specifically, the TRS and the EMPS served as real-world plants, showcasing the efficacy of the N-SPSA in minimizing objective functions with the lowest standard deviation as compared to other algorithms. Notably, both the N-SPSA and the NL-SPSA have exceeded the AMVO-SCA in the accurate modeling of the TRS and the EMPS under a smaller number of NFEs. Moreover, on account of a lower mean and worst value, the N-SPSA further outperformed the NL-SPSA in Wilcoxon's rank-sum test to establish precise response identification for the objective functions. The introduced algorithmic modifications through the N-SPSA offer promising prospects for mitigating limitations inherent in the conventional SPSA-based method.

While the proposed method offers numerous advantages, it's important to note that selecting optimal values for the N-SPSA coefficients can be challenging and may require considerable effort, despite the guidelines provided in the original SPSA research paper. The performance of the N-SPSA can be influenced by specific tuning parameters, including step size and perturbation sizes, and these factors can significantly affect the algorithm's effectiveness. Meanwhile, future research directions could explore the applicability of the N-SPSA in the parameter identification of diverse nonlinear block-oriented models such as Wiener models, Hammerstein-Wiener models, as well as multi-input multi-output (MIMO) variants. Furthermore, the N-SPSA could also be practically applied as a data-driven tool in fine-tuning various controllers, such as proportional-integral-derivative controllers, fuzzy logic controllers, neuro-fuzzy controllers and others.

## CRediT authorship contribution statement

**Nik Mohd Zaitul Akmal Mustapha:** Writing – original draft. **Mohd Ashraf Ahmad:** Supervision, Funding acquisition.

## Declaration of competing interest

The authors declare that they have no known competing financial interests or personal relationships that could have appeared to influence the work reported in this paper.

## Acknowledgement

In-depth appreciation is advanced for monetary support given by University Malaysia Pahang Al-Sultan Abdullah through the Distinguished Research Grant RDU223011.

## Supplementary materials

Supplementary material associated with this article can be found, in the online version, at doi:10.1016/j.ijcce.2025.04.004.

## References

Abdulsadda, A. T., & Iqbal, K. (2011). An improved SPSA algorithm for system identification using fuzzy rules for training neural networks. *International The Journal of Automation and Computing, 8*(3), 333–339. https://doi.org/10.1007/s11633-011-0589-x

Ahmad, M. A., Azuma, S. I., & Sugie, T. (2016). Identification of continuous-time Hammerstein systems by simultaneous perturbation stochastic approximation. *Expert Systems with Applications, 43*, 51–58. https://doi.org/10.1016/j.eswa.2015.08.041

Ahmad, M. A., Mustapha, N. M. Z. A., Nasir, A. N. K., Tumari, M. Z. M., Ismail, R. M. T. R., & Ibrahim, Z. (2018). Using normalized simultaneous perturbation stochastic approximation for stable convergence in model-free control scheme. *Proceedings of 4th IEEE International Conference on Applied System Innovation 2018, ICASI 2018*, 935–938. https://doi.org/10.1109/ICASI.2018.8394422

Aji, G. K., Hatou, K., & Morimoto, T. (2020). Modeling the dynamic response of plant growth to root zone temperature in hydroponic chili pepper plant using neural networks. *Agriculture (Switzerland), 10*(6), 1–14. https://doi.org/10.3390/agriculture10060234

Akramizadeh, A., Farjami, A. A., & Khaloozadeh, H. (2002). Nonlinear Hammerstein model identification using genetic algorithm. In *Proceedings - 2002 IEEE International Conference on Artificial Intelligence Systems, ICAIS 2002* (pp. 351–356). https://doi.org/10.1109/ICAIS.2002.1048126

Aljamaan, I. A., Al-Dhaifallah, M. M., & Westwick, D. T. (2021). Hammerstein Box-Jenkins System identification of the cascaded tanks benchmark system. *Mathematical Problems in Engineering, 2021*. https://doi.org/10.1155/2021/6613425

Alonge, F., Rabbeni, R., Pucci, M., & Vitale, G. (2015). Identification and robust control of a quadratic DC/DC boost converter by Hammerstein model. *IEEE Transactions on Industry Applications, 51*(5), 3975–3985. https://doi.org/10.1109/TIA.2015.2416154

Antoniou, C., Azevedo, C. L., Lu, L., Pereira, F., & Ben-Akiva, M. (2015). W-SPSA in practice: Approximation of weight matrices and calibration of traffic simulation models. *Transportation Research; a journal of science and its applications Procedia, 7*, 233–253. https://doi.org/10.1016/j.trpro.2015.06.013

Azim, M. A., Aung, Z., Xiao, W., Khadkikar, V., & Jamalipour, A. (2012). Localization in wireless sensor networks by constrained simultaneous perturbation stochastic approximation technique. In *6th International Conference on Signal Processing and*

*Communication Systems, ICSPCS 2012 - Proceedings*. https://doi.org/10.1109/ICSPCS.2012.6507961

Bai, E. W., & Li, K. (2010). Convergence of the iterative algorithm for a general Hammerstein system identification. *Automatica, 46*(11), 1891–1896. https://doi.org/10.1016/j.automatica.2010.07.007

Baldelli, D. H., & Lind, R. (2005). Nonlinear aeroelastic/aeroservoelastic modeling by block-oriented identification. *The Journal of Guidance and Dynamics (Pembroke, Ont.), 28*(5), 1056–1064. https://doi.org/10.2514/1.11792

Bao, Y., Wang, L. Y., Wang, C., & Wang, Y. (2018). Hammerstein models and real-time system identification of load dynamics for voltage management. *IEEE access : Practical innovations, open solutions, 6*, 34598–34607. https://doi.org/10.1109/ACCESS.2018.2849002

Brunot, M., Janot, A., Carrillo, F., Garnier, H., Vandanjon, P. O., & Gautier, M. (2015). Physical parameter identification of a one-degree-of-freedom electromechanical system operating in closed loop. *IFAC-PapersOnLine, 48*(28), 823–828. https://doi.org/10.1016/j.ifacol.2015.12.231

Chidume, C. E., & Djitté, N. (2013). An iterative method for solving nonlinear integral equations of Hammerstein type. *Applied Mathematics and Computation, 219*(10), 5613–5621. https://doi.org/10.1016/j.amc.2012.11.051

D, E.C.P., Daniel, A., & Marco, P. (2018). *Nonlinear system identification based on ANFIS-Hammerstein model using gravitational search algorithm*. 182–203. doi:10.1007/s10489-017-0969-1.

Ding, F., Chen, H., Xu, L., Dai, J., Li, Q., & Hayat, T. (2018). A hierarchical least squares identification algorithm for Hammerstein nonlinear systems using the key term separation. *The Journal of the Franklin Institute, 355*(8), 3737–3752. https://doi.org/10.1016/j.jfranklin.2018.01.052

Ding, F., Liu, X., & C, J. (2013). Gradient-based and least-squares-based iterative algorithms for Hammerstein.Pdf. *IET Control Theory and Applications* (pp. 176–184). https://doi.org/10.1049/iet-cta.2012.0313

Fard, R. D., Karrari, M., & Malik, O. P. (2005). Synchronous generator model identification for control application using volterra series. *IEEE Transactions on Energy Conversion, 20*(4), 852–858. https://doi.org/10.1109/TEC.2005.847997

Gogula, S., & Vakula, V. S. (2024). Multi-objective Harris Hawks optimization algorithm for selecting best location and size of distributed generation in radial distribution system. *International The Journal of Cognitive Computing in Engineering, 5*, 436–452. https://doi.org/10.1016/j.ijcce.2024.08.003

Gómez, J. C., & Baeyens, E. (2004). Identification of block-oriented nonlinear systems using orthonormal bases. *The Journal of Process Control, 14*(6), 685–697. https://doi.org/10.1016/j.jprocont.2003.09.010

Gotmare, A., Patidar, R., & George, N. V. (2015). Nonlinear system identification using a cuckoo search optimized adaptive Hammerstein model. *Expert Systems With Applications, 42*(5), 2538–2546. https://doi.org/10.1016/j.eswa.2014.10.040

Haber, A., & Verhaegen, M. (2020). Modeling and state-space identification of deformable mirrors. *Optics Express, 28*(4), 4726. https://doi.org/10.1364/oe.382880

Hacioğlu, R., & Williamson, G. A. (2001). Reduced complexity Volterra models for nonlinear system identification. *Eurasip The Journal on Applied Signal Processing, 2001*(4), 257–265. https://doi.org/10.1155/S1110865701000324

Hammar, K., Djamah, T., & Bettayeb, M. (2017). Pso based on the key-term separation principle for fractional hammerstein system identification. In *2017 5th International Conference on Electrical Engineering - Boumerdes, ICEE-B 2017* (pp. 29–31). https://doi.org/10.1109/ICEE-B.2017.8192115

Hatanaka, T. (2001). Hammerstein model identification method based on genetic programming. In *Proceedings of the 2001 Congress on Evolutionary Computation (IEEE Cat. No.01TH8546)* (pp. 1431–1435).

He, F., Wei, H. L., & Billings, S. A. (2015). Identification and frequency domain analysis of non-stationary and nonlinear systems using time-varying NARMAX models. *International The Journal of Systems Science (New York, N.Y.), 46*(11), 2087–2100. https://doi.org/10.1080/00207721.2013.860202

Hou, J., Chen, F., Li, P., & Zhu, Z. (2020). Gray-box parsimonious subspace identification of Hammerstein-type systems. *IEEE Transactions on Industrial Electronics, 0046*(c). https://doi.org/10.1109/tie.2020.3026286

Islam, M. S., Ahmad, M. A., & Wen, C. B. (2024). Identification of continuous-time Hammerstein model using improved Archimedes optimization algorithm. *International The Journal of Cognitive Computing in Engineering, 5*, 475–493. https://doi.org/10.1016/j.ijcce.2024.09.004

Jafari, M., Salimifard, M., & Dehghani, M. (2014). Identification of multivariable nonlinear systems in the presence of colored noises using iterative hierarchical least squares algorithm. *ISA Transactions, 53*(4), 1243–1252. https://doi.org/10.1016/j.isatra.2013.12.034

Spall, James C (1992). Multivariate stochastic approximation using a simultaneous pertubation gradient approximation. *IEEE Transactions on Automatic Control, 37*(3), 332–341. Issue.

Janjanam, L., Saha, S. K., Kar, R., & Mandal, D. (2021). Global gravitational search algorithm-aided Kalman filter design for volterra-based nonlinear system identification. *Circuits, Systems, and Signal Processing, 40*(5), 2302–2334. https://doi.org/10.1007/s00034-020-01593-6

Janot, A., Gautier, M., & Brunot, M. (2019). Data set and reference models of EMPS. *Nonlinear System Identification Benchmarks*. https://hal.archives-ouvertes.fr/hal-02178709/.

Janot, Alexandre, Young, P. C., & Gautier, M. (2017). Identification and control of electro-mechanical systems using state-dependent parameter estimation. *International The Journal of Control, 90*(4), 643–660. https://doi.org/10.1080/00207179.2016.1209565

Jin, Q., & Cui, M. (2020). Chaotic salp swarm algorithm: Application to parameter identification for MIMO Hammerstein model under heavy tail noise. *Proceedings - 2020 12th International Conference on Intelligent Human-Machine Systems and Cybernetics, IHMSC, 2020*(2), 264–268. https://doi.org/10.1109/IHMSC49165.2020.00066. *1*.

Jui, J. J., & Ahmad, M. A. (2021). A hybrid metaheuristic algorithm for identification of continuous-time Hammerstein systems. *Applied Mathematical Modelling, 95*, 339–360. https://doi.org/10.1016/j.apm.2021.01.023

Kelly, N., & Zhu, A. (2018). Direct error-searching SPSA-based model extraction for digital predistortion of RF power amplifiers. *IEEE Transactions on Microwave Theory and Techniques, 66*(3), 1512–1523. https://doi.org/10.1109/TMTT.2017.2748128

Kong, X., Guo, J., Zheng, D., Zhang, J., & Fu, W. (2020). Quality control for medium voltage insulator via a knowledge-informed spsa based on historical gradient approximations. *Processes, 8*(2). https://doi.org/10.3390/pr8020146

Kostic, B., Gentile, G., & Antoniou, C. (2017). Techniques for improving the effectiveness of the SPSA algorithm in dynamic demand calibration. In *5th IEEE International Conference on Models and Technologies for Intelligent Transportation Systems, MT-ITS 2017 - Proceedings* (pp. 368–373). https://doi.org/10.1109/MTITS.2017.8005699

Kumon, T., Iwasaki, M., Suzukir, T., & Hashiyama, T. (2000). *Nonlinear System Identification Using Genetic Algorithm* (pp. 2485–2491). https://doi.org/10.1109/IECON.2000.972387

Le, F., Markovsky, I., Freeman, C. T., & Rogers, E. (2012). Recursive identification of Hammerstein systems with application to electrically stimulated muscle. *Control Engineering Practice, 20*(4), 386–396. https://doi.org/10.1016/j.conengprac.2011.08.001

Li, G., & Wen, C. (2011). Convergence of normalized iterative identification of Hammerstein systems. *Systems & Control Letters, 60*(11), 929–935. https://doi.org/10.1016/j.sysconle.2011.07.010

Li, J. (2013). Parameter estimation for Hammerstein CARARMA systems based on the Newton iteration. *Applied Mathematics Letters, 26*(1), 91–96. https://doi.org/10.1016/j.aml.2012.03.038

Liu, L., Zhu, C., Liu, Y. J., Wang, R., & Tong, S. (2023). Performance improvement of active suspension constrained system via neural network identification. *IEEE Transactions on Neural Networks and Learning Systems, 34*(10), 7089–7098. https://doi.org/10.1109/TNNLS.2021.3137883

Liu, X., & Yang, X. (2022). Identification of nonlinear State-space systems with skewed measurement noises. *IEEE Transactions on Circuits and Systems I: Regular Papers, 69*(11), 4654–4662. https://doi.org/10.1109/TCSI.2022.3193444

Mao, Y., & Ding, F. (2014). Multi-innovation stochastic gradient identification for Hammerstein controlled autoregressive autoregressive systems based on the filtering technique. *Nonlinear Dynamics (Pembroke, Ont.), 79*(3), 1745–1755. https://doi.org/10.1007/s11071-014-1771-9

Mao, Y., & Ding, F. (2016). A novel parameter separation based identification algorithm for Hammerstein systems. *Applied Mathematics Letters, 60*, 21–27. https://doi.org/10.1016/j.aml.2016.03.016

Masti, D., & Bemporad, A. (2021). Learning nonlinear state–space models using autoencoders. *Automatica, 129*, Article 109666. https://doi.org/10.1016/j.automatica.2021.109666

Mehmood, A., Chaudhary, N. I., Zameer, A., & Raja, M. A. Z. (2019). Backtracking search optimization heuristics for nonlinear Hammerstein controlled auto regressive auto regressive systems. *ISA Transactions, 91*, 99–113. https://doi.org/10.1016/j.isatra.2019.01.042

Mehmood, A., Zameer, A., Chaudhary, N. I., Ling, S. H., & Raja, M. A. Z. (2020). Design of meta-heuristic computing paradigms for Hammerstein identification systems in electrically stimulated muscle models. *Neural Computing and Applications, 32*(16), 12469–12497. https://doi.org/10.1007/s00521-020-04701-4

Mete, S., Ozer, S., & Zorlu, H. (2016). System identification using Hammerstein model optimized with differential evolution algorithm. *AEU - International The Journal of Electronics and Communications, 70*(12), 1667–1675. https://doi.org/10.1016/j.aeue.2016.10.005

Misyris, G. S., Venzke, A., & Chatzivasileiadis, S. (2020). Physics-informed neural networks for power systems. In *IEEE Power and Energy Society General Meeting*. https://doi.org/10.1109/PESGM41954.2020.9282004

Mok, R. H., & Ahmad, M. A. (2024). Smoothed functional algorithm with norm-limited update vector for identification of continuous-time fractional-order Hammerstein models. *IETE The Journal of Research; a journal of science and its applications*. https://doi.org/10.1080/03772063.2022.2152879

Mustapha, N. M. Z. A., Suid, M. H., Raja Ismail, R. M. T., Nasir, A. N. K., Ahmad, M. A., Mohd Tumari, M. Z., & Jui, J. J. (2019). A data-driven PID controller for flexible joint manipulator using normalized simultaneous perturbation stochastic approximation. *The Journal of Advanced Manufacturing Technology (Elmsford, N.Y.), 13*(2), 143–154.

Ozer, S., Zorlu, H., & Mete, S. (2016). System identification application using Hammerstein model. *Sadhana - Academy Proceedings in Engineering Sciences, 41*(6), 597–605. https://doi.org/10.1007/s12046-016-0505-8

Pal, P. S., Ghosh, A., Choudhury, S., Debapriya, D., Kar, R., Mandal, D., & Ghoshal, S. P. (2016a). Identification of Hammerstein model using bacteria foraging optimization algorithm. *International Conference on Communication and Signal Processing, ICCSP 2016*, 1609–1613. https://doi.org/10.1109/ICCSP.2016.7754432

Pal, P. S., Ghosh, A., Choudhury, S., Kumar, A., Kar, R., Mandal, D., & Ghoshal, S. P. (2016b). Hammerstein model based system identification using craziness based particle swarm optimization algorithm. *International Conference on Communication and Signal Processing, ICCSP, 2016*, 1623–1627. https://doi.org/10.1109/ICCSP.2016.7754436

Panda, A., & Pani, S. (2016). A WNN model trained with orthogonal colliding bodies optimization for accurate identification of hammerstein plant. In *2016 IEEE Congress on Evolutionary Computation, CEC 2016* (pp. 1100–1106). https://doi.org/10.1109/CEC.2016.7743911

Pouladi, B., Karkevandi-Talkhooncheh, A., Sharifi, M., Gerami, S., Nourmohammad, A., & Vahidi, A. (2020). Enhancement of SPSA algorithm performance using reservoir quality maps: Application to coupled well placement and control optimization problems. *The Journal of Petroleum Science (New York, N.Y.) and Engineering, 189*, Article 106984. https://doi.org/10.1016/j.petrol.2020.106984

Qurashi, M., Ma, T., Chaniotakis, E., & Antoniou, C. (2020). PC-SPSA: Employing dimensionality reduction to limit SPSA search noise in DTA model calibration. *IEEE Transactions on Intelligent Transportation Systems, 21*(4), 1635–1645. https://doi.org/10.1109/TITS.2019.2915273

Rădac, M. B., Precup, R. E., Petriu, E. M., & Preitl, S. (2011). Application of IFT and SPSA to servo system control. *IEEE Transactions on Neural Networks, 22*(12 PART 2), 2363–2375. https://doi.org/10.1109/TNN.2011.2173804

Raja, M. A. Z., Shah, A. A., Mehmood, A., Chaudhary, N. I., & Aslam, M. S. (2018). Bio-inspired computational heuristics for parameter estimation of nonlinear Hammerstein controlled autoregressive system. *Neural Computing and Applications, 29*(12), 1455–1474. https://doi.org/10.1007/s00521-016-2677-x

Ramachandran, A., & Sangaiah, A. K. (2021). A review on object detection in unmanned aerial vehicle surveillance. *International The Journal of Cognitive Computing in Engineering, 2*, 215–228. https://doi.org/10.1016/j.ijcce.2021.11.005

Ros-Roca, X., Montero, L., Schneck, A., & Barceló, J. (2018). Investigating the performance of SPSA in simulation-optimization approaches to transportation problems. *Transportation Research; a journal of science and its applications Procedia, 34*, 83–90. https://doi.org/10.1016/j.trpro.2018.11.017

Saat, S., Ahmad, M. A., & Ghazali, M. R. (2025). Data-driven brain emotional learning-based intelligent controller-PID control of MIMO systems based on a modified safe experimentation dynamics algorithm. *International The Journal of Cognitive Computing in Engineering, 6*, 74–99. https://doi.org/10.1016/j.ijcce.2024.11.005

Saleem, A., Mesbah, M., & Al-Ratout, S. (2017). Nonlinear hammerstein model identification of amplified piezoelectric actuators (APAs): Experimental considerations. In *2017 4th International Conference on Control, Decision and Information Technologies, CoDIT 2017* (pp. 633–638). https://doi.org/10.1109/CoDIT.2017.8102665

Salhi, H., & Kamoun, S. (2015). A recursive parametric estimation algorithm of multivariable nonlinear systems described by Hammerstein mathematical models. *Applied Mathematical Modelling, 39*(16), 4951–4962. https://doi.org/10.1016/j.apm.2015.03.050

Schoukens, J., Pintelon, R., Rolain, Y., Schoukens, M., Tiels, K., Vanbeylen, L., Van Mulders, A., & Vandersteen, G. (2015). Structure discrimination in block-oriented models using linear approximations: A theoretic framework. *Automatica, 53*, 225–234. https://doi.org/10.1016/j.automatica.2014.12.045

Schoukens, M., & Tiels, K. (2017). Identification of block-oriented nonlinear systems starting from linear approximations: A survey. *Automatica, 85*, 272–292. https://doi.org/10.1016/j.automatica.2017.06.044

Sharma, S., Gupta, R., Bhatia, R., Toor, A. P., & Setia, H. (2021). Predicting microbial response to anthropogenic environmental disturbances using artificial neural network and multiple linear regression. *International The Journal of Cognitive Computing in Engineering, 2*, 65–70. https://doi.org/10.1016/j.ijcce.2021.03.001

Shi, H. L., Cai, Y. L., & Qiu, Z. L. (2006). System identification based on NARMAX model using Hopfield networks. *The Journal of Shanghai University, 10*(3), 238–243. https://doi.org/10.1007/s11741-006-0122-6

Shi, X., & Zhang, H. T. (2016). Modeling of based pneumatics muscle actuator (PMA) on hammerstein system. *Chinese Control Conference, CCC*, 2279–2284. https://doi.org/10.1109/ChiCC.2016.7553706

Tanaka, Y., Azuma, S. I., & Sugie, T. (2015). Simultaneous perturbation stochastic approximation with norm-limited update vector. *Asian The Journal of Control, 17*(6), 2083–2090. https://doi.org/10.1002/asjc.1153

Toha, S. F., Julai, S., & Tokhi, M. O. (2012). *Ant Colony Based Model Prediction of a Twin Rotor System, 41* pp. 1135–1144). https://doi.org/10.1016/j.proeng.2012.07.293

Tympakianaki, A., Koutsopoulos, H. N., & Jenelius, E. (2015). c-SPSA: Cluster-wise simultaneous perturbation stochastic approximation algorithm and its application to dynamic origin-destination matrix estimation. *Transportation Research; A journal of science and its applications Part C: Emerging Technologies, 55*, 231–245. https://doi.org/10.1016/j.trc.2015.01.016

Tympakianaki, A., Koutsopoulos, H. N., & Jenelius, E. (2018). Robust SPSA algorithms for dynamic OD matrix estimation. *Procedia Computer Science (New York, N.Y.), 130*, 57–64. https://doi.org/10.1016/j.procs.2018.04.012

Wang, D. (2016). Hierarchical parameter estimation for a class of MIMO Hammerstein systems based on the reframed models. *Applied Mathematics Letters, 57*, 13–19. https://doi.org/10.1016/j.aml.2015.12.018

Wang, D. Q., Liu, H. B., & Ding, F. (2015). Highly efficient identification methods for dual-rate Hammerstein systems. *IEEE Transactions on Control Systems Technology (Elmsford, N.Y.), 23*(5), 1952–1960. https://doi.org/10.1109/TCST.2014.2387216

Wang, D., & Zhang, W. (2015). Improved least squares identification algorithm for multivariable Hammerstein systems. *The Journal of the Franklin Institute, 352*(11), 5292–5307. https://doi.org/10.1016/j.jfranklin.2015.09.007

Xu, S., Li, J., Gu, J., Hua, L., & Shang, L. (2020). Parameter estimation of Hammerstein systems based on the gravitational search algorithm. In *Proceedings of the 32nd Chinese Control and Decision Conference, CCDC 2020* (pp. 1708–1713). https://doi.org/10.1109/CCDC49329.2020.9164158

Yan, J., & Deller, J. R. (2016). NARMAX model identification using a set-theoretic evolutionary approach. *Signal Processing, 123*, 30–41. https://doi.org/10.1016/j.sigpro.2015.12.001

Yang, N., & Jin, Q. (2017). A modified BBO algorithm and its application for identifying Hammerstein system under heavy-tailed noises. In *ICAC 2017 - 2017 23rd IEEE International Conference on Automation and Computing: Addressing Global Challenges through Automation and Computing*. https://doi.org/10.23919/IConAC.2017.8082040

Zhang, Q., Wang, Q., & Li, G. (2016). Nonlinear modeling and predictive functional control of Hammerstein system with application to the turntable servo system. *Mechanical Systems and Signal Processing, 72–73*, 383–394. https://doi.org/10.1016/j.ymssp.2015.09.011

Zimmerschied, R., & Isermann, R. (2009). Nonlinear system identification of block-oriented systems using local affine models. In *, 42. IFAC Proceedings Volumes*. IFAC. https://doi.org/10.3182/20090706-3-fr-2004.00109. Issue.

Zorlu, H., Mete, S., & Ozer, S. (2018). System identification using Hammerstein model optimized with artifical Bee Colony algorithm. *Ömer Halisdemir Üniversitesi Mühendislik Bilimleri Dergisi, 7*(1), 83–98. https://doi.org/10.28948/ngumuh.386351